

Towards Implementable Quantum Divide-and-Conquer: A TSP Solver with Improved Exponential Base over Held–Karp

Xujun Bai^{1,2}, Yun Shang^{1,3,†,*}, and Honghong Lin^{1,2}

¹*Institute of Mathematics, Academy of Mathematics and Systems Science,
Chinese Academy of Sciences, Beijing 100190, China*

²*School of Mathematical Sciences, University of Chinese Academy of Sciences,
Chinese Academy of Sciences, Beijing, 100049, China*

³*State Key Laboratory of Mathematical Sciences,
Academy of Mathematics and Systems Science,
Chinese Academy of Sciences, Beijing, 100190, China*

The traveling salesman problem (TSP) is a significant classical NP-hard combinatorial optimization problem. In this work, we demonstrate that combining classical dynamic programming with quantum search can yield an achievable quantum advantage for TSP on the basis of excellent work by the authors of [1]. We design the quantum divide-and-conquer strategy to provide a parameterized spectrum for this combination. The hybrid algorithm proposed in [1] corresponds to a specific case in this spectrum, while the two extremes of the spectrum represent the purely classical Held-Karp and the purely quantum search algorithm, respectively. Within our parameterized spectrum, we prove that the optimal query complexity is $O^*(1.865666\dots^n)$, achieved with the 4-subset scheme, while the counting in [1] overlooked half of the recursive branches. The correct query complexity of their algorithm is $O^*(2.225880\dots^n)$ at their chosen parameter ($\alpha \approx 0.055362$), and cannot fall below $O^*(2^n)$ for any α — meaning their 8-subset scheme, correctly analyzed, never surpasses the classical Held-Karp bound.

Furthermore, in previous studies on quantum advantages for NP-hard combinatorial optimization problems, researchers focused only on improvements in query complexity. Our work, however, points out that the quantum advantage stems not only from the quadratic speedup of quantum search but also from the structured quantum state preparation. We argue that structured state preparation is indispensable for realizing the oracle operator while maintaining the total time complexity of $O^*(1.865666\dots^n)$. Therefore, we design an elegant method for preparing the set partition state, which makes our TSP solver practically executable.

Keywords: quantum divide-and-conquer, ordered set partition, quantum search, traveling salesman problem (TSP)

[†] shangyun@amss.ac.cn

* Corresponding authors

I. INTRODUCTION

In classical computing, dynamic programming is a cornerstone algorithmic technique that provides structured solutions to problems with overlapping subproblems and optimal substructure. TSP is an important example of dynamic programming [2, 3]. As an NP-hard combinatorial optimization problem with theoretical significance and applied merit, TSP has been thoroughly studied in terms of both exact and approximation algorithms [4]. Special cases, such as TSP on cubic graphs, can achieve excellent complexity bounds [5]. In the quantum field, algorithms offering quantum speedups for bounded-degree graphs [6, 7] and for classical dynamic programming [1] have also been deeply investigated. The query complexity of $O^*(1.727391\dots^n)$ by the authors of [1] is a significant result because it is suitable for general TSP. However, we can prove that this result does not account for the entire solution space. We will explain what their calculation overlooked from the perspective of ordered set partition. Inspired by this insight, we design a quantum divide-and-conquer strategy. Based on this strategy, we demonstrate that combining classical dynamic programming with quantum search can yield an achievable quantum advantage for TSP. We provide a parameterized spectrum for this combination. The hybrid algorithm proposed in [1] corresponds to a specific case in this spectrum, while the two extremes of the spectrum represent the purely classical Held-Karp and the purely quantum search algorithm, respectively. We prove that the counting in [1] overlooked half of the recursive branches; the correct query complexity of their algorithm is $O^*(2.225880\dots^n)$ at their chosen parameter ($\alpha \approx 0.055362$), and cannot fall below $O^*(2^n)$ for any α — meaning their 8-subset scheme, correctly analyzed, never surpasses the classical Held-Karp bound. Within our parameterized spectrum, the optimal query complexity is $O^*(1.865666\dots^n)$, achieved with the 4-subset scheme.

For the implementation of our quantum divide-and-conquer strategy, the construction and execution of the oracle constitute a major challenge. Although some studies have explored oracles by phase kick-back [8, 9], robust quantum minimum finding in noisy settings [10], quantum search using weak measurements [11], recursive oracle expansion [12] and oracles constructed by spinorial representations [13], the construction of the oracle in practice is highly challenging due to its problem dependence. We cleverly shift the difficulty of oracle construction to state preparation. This represents a further application of the oracle design principle from the previous work [14]. In that work, the authors divided the qubits into the index and value registers. By preparing the uniform superposition state of all Hamiltonian cycles of order n in the index register, they could use techniques such as a shortcut of quantum Fourier transform (QFT) [15] to conveniently compute the corresponding data into the value register.

The quantum superposition state of combinatorial objects can be leveraged to design quantum search, quantum walk [16] and quantum variation algorithms [17] for combinatorial optimization problems. Examples include employing Dicke states to solve the vertex cover problem [18], utilizing the superposition state of Hamiltonian cycles to address TSP [14] and permutations for graph comparison [19], etc. In this work, we generalize the preparation method for Dicke states to enable the preparation of uniform superposition states over ordered set partitions with labels. We argue that structured state preparation is indispensable for realizing the oracle operator while maintaining the total time complexity of $O^*(1.865666\dots^n)$. Using our state preparation method, we can access classical data and compute the lengths of Hamiltonian cycles corresponding to ordered set partitions with labels into the value register using the sparse Boolean memory (SBM) [20]. Our TSP solver is practically executable, maintaining the total time complexity of $O^*(1.865666\dots^n)$. To demonstrate the performance of our TSP solver, we conducted simulation experiments on small instances using IBM's Qiskit. Due to the qubit limitation of the simulator, we replaced the SBM with the shortcut of QFT in the simulation experiments.

II. QUANTUM DIVIDE-AND-CONQUER

A. Revisit the Algorithm for TSP in [1]

Let $A = (\omega_{ij})_{n \times n} \in \mathbf{R}^{n \times n}$ be the weighted adjacency matrix of the complete undirected graph $G = (V, E)$ and $f(u, S)$ denote the cost of the shortest route that starts from $u \notin S$ and passes through each vertex in $S \subset V$ exactly once. The best known classical dynamic programming algorithm for TSP is provided as **Algorithm 1** [2, 21], the time complexity of which is $O(n^2 2^n)$.

Algorithm 1 The classical dynamic programming for TSP.

Input: The weighted adjacency matrix $A = (\omega_{ij})_{n \times n}$. A special vertex that the salesman starts from, here we select $0 \in V$.

Output: The shortest Hamiltonian cycle that starts and ends at the vertex 0 and its cost.

- 1: For all vertices $u \neq 0$, set $f(u, \emptyset) = \omega_{0u}$.
 - 2: **for** $k = 1$ to $n - 1$ **do**
 - 3: **if** $k < n - 1$ **then**
 - 4: $\forall S \subset V \setminus \{0\}$ where $|S| = k$, $\forall u \in V \setminus (S \cup \{0\})$, calculate $f(u, S) = \min_{t \in S} \{f(t, S \setminus \{t\}) + \omega_{ut}\}$. Record the minimizer t^* .
 - 5: **else**
 - 6: For $S = V \setminus \{0\}$, calculate the cost of the shortest Hamiltonian cycle of the graph G : $f(0, S) = \min_{t \in S} \{f(t, S \setminus \{t\}) + \omega_{t0}\}$. Record the minimizer t^* .
 - 7: **end if**
 - 8: **end for**
 - 9: Trace back through the DP table to retrieve the shortest Hamiltonian cycle.
-

The recursive formulas for TSP used in [1] are

$$f(S, u, v) = \min_{\substack{t \in N(u) \cap S \\ t \neq v}} \{f(S \setminus \{u\}, t, v) + \omega_{ut}\}, \quad f(\{v\}, v, v) = 0, \quad (1)$$

$$f(S, u, v) = \min_{\substack{X \subset S, |X|=k \\ u \in X, v \notin X}} \min_{\substack{t \in X \\ t \neq u}} \{f(X, u, t) + f((S \setminus X) \cup \{t\}, t, v)\}, \quad (2)$$

$$f(V) = \min_{\substack{S \subset V \\ |S| = \frac{n}{2}}} \min_{\substack{u, v \in S \\ u \neq v}} \{f(S, u, v) + f((V \setminus S) \cup \{u, v\}, v, u)\}, \quad (3)$$

where $f(S, u, v)$ denotes the minimum cost of the routes that pass through all vertices in S exactly once starting at $u \in S$ and ending at $v \in S$, $f(V)$ denotes the cost of the shortest Hamiltonian cycle of G , and $N(u)$ is the set of neighborhoods of u . The algorithm proposed in [1] is provided as **Algorithm 2**.

Algorithm 2 The hybrid dynamic programming for TSP.

Input: The weighted adjacency matrix $A = (\omega_{ij})_{n \times n}$. Let $\alpha \leq 1/2$ to ensure $\alpha n/4 \leq (1 - \alpha)n/4$.

Output: The shortest Hamiltonian cycle and its cost.

- 1: Calculate $f(S, u, v)$ for all $|S| \leq (1 - \alpha)n/4$ classically using the formula (1) and load them in QRAM (quantum random access memory).
 - 2: Run quantum minimum finding over all subsets $S \subset V$ where $|S| = n/2$ to calculate the answer $f(V)$ using the formula (3). To calculate $f(S, u, v)$ for all $|S| = n/2$, run quantum minimum finding using the formula (2) with $k = n/4$. To calculate $f(S, u, v)$ for all $|S| = n/4$, run quantum minimum finding using the formula (2) with $k = \alpha n/4$. For $|S| = \alpha n/4$ or $|S| = (1 - \alpha)n/4$, query QRAM.
-

The classical step 1 of **Algorithm 2** requires the complexity of

$$O^* \left(\binom{n}{\leq (1-\alpha)n/4} \right) = O^*(2^{H(\frac{1-\alpha}{4})n}). \quad (4)$$

Counting the number of distinct subset selection at step 2 of **Algorithm 2**, the authors of [1] derive the query complexity of the quantum part as

$$O^* \left(\sqrt{\binom{n}{n/2} \binom{n/2}{n/4} \binom{n/4}{\alpha n/4}} \right) = O^*(2^{\frac{1}{2}(1+\frac{1}{2}+\frac{H(\alpha)}{4})n}). \quad (5)$$

In formulas (4) and (5), O^* indicates ignoring the polynomial factors, and the entropy approximation is used:

$$\begin{aligned} \binom{n}{k} &\leq 2^{nH(k/n)}, \\ \binom{n}{\leq k} &= \sum_{i=0}^k \binom{n}{i} \leq 2^{nH(k/n)}, \end{aligned} \quad (6)$$

where $H(\epsilon) = -[\epsilon \log_2 \epsilon + (1-\epsilon) \log_2 (1-\epsilon)]$, $\epsilon \in [0, 1]$ is the binary entropy. The authors of [1] argued that the overall complexity is minimized when the complexities of the classical part and the quantum part are equal, which gives the optimal $\alpha \approx 0.055362$ and the corresponding complexity of **Algorithm 2** is $O^*(1.727391 \dots^n)$. This result is better than the best known classical complexity of $O(n^2 2^n)$ given by **Algorithm 1**. However, we will prove that this complexity is unattainable because it does not account for the entire solution space.

Theorem 1. *The number of solutions that the oracle of the quantum part in **Algorithm 2** must traverse is*

$$N = O^* \left(\binom{n}{n/2} \binom{n/2}{n/4}^2 \binom{n/4}{\alpha n/4}^4 \right), \quad (7)$$

not the $O^* \left(\binom{n}{n/2} \binom{n/2}{n/4} \binom{n/4}{\alpha n/4} \right)$ counted by the authors of [1]. Under Grover's algorithm [22], quantum minimum finding requires $O(\sqrt{N})$ queries, yielding the correct query complexity

$$O(\sqrt{N}) = O^* \left(2^n \binom{n/4}{\alpha n/4}^2 \right) = O^*(2^{n(1+H(\alpha)/2)}). \quad (8)$$

For the parameter $\alpha \approx 0.055362$ chosen by the authors of [1], this evaluates to $O^*(2.225880 \dots^n)$, which exceeds the classical Held-Karp bound of $O^*(2^n)$. In fact, the corrected quantum part satisfies $O(\sqrt{N}) > O^*(2^n)$ for any valid $\alpha > 0$, meaning the 8-subset scheme of [1] cannot surpass Held-Karp after the counting is corrected.

The proof of **Theorem 1** can be found in **Appendix A**. The quantum advantage of Grover's search framework requires that quantum minimum finding can be executed in a single coherent process. Therefore, the oracle must be capable of concatenating all partial paths into complete solutions in order to mark them correctly. This requirement for the oracle's ability to concatenate paths naturally leads to the quantum divide-and-conquer algorithm that we will introduce next.

B. Divide-and-Conquer

The four subsets represented by four colored nodes drawn at level 2 in **Figure A1** constitute a partition of the entire set, and $\binom{n}{n/2} \binom{n/2}{n/4}^2 = \frac{n!}{[(n/4)!]^4}$ is exactly the number of ways to partition a set into four disjoint subsets of equal size in order, which inspires us to design a quantum divide-and-conquer algorithmic framework for solving TSP.

Let $A = (\omega_{ij})_{n \times n} \in \mathbf{R}^{n \times n}$ be the weighted adjacency matrix of the complete undirected graph $G = (S, E)$. Divide the n -vertex set S into k disjoint subsets S_i of sizes m_1, m_2, \dots, m_k respectively to get an ordered k -partition, where $\sum_{i=1}^k m_i = n$ and the order of subsets is taken into account. Fix arbitrary two vertices of each subset as origin and end, denoted by u_i, v_i .

Lemma 1. *Let L_i denote the shortest path from u_i to v_i that passes through all vertices in S_i exactly once. Concatenate these paths into a cycle by adding edges $v_1 u_2, v_2 u_3, \dots, v_{k-1} u_k, v_k u_1$. Let all these cycles formed by all possible ordered k -partitions with sizes m_1, m_2, \dots, m_k and all possible selections of u_i, v_i for fixed S_i constitute a set P , then the shortest Hamiltonian cycle belongs to P .*

The proof of **Lemma 1** can be found in **Appendix B. Lemma 1** suggests that we can first get all shortest paths of subsets by classical dynamic programming and then search for the shortest Hamiltonian cycle over the components of the uniform superposition state encoding all elements of P . Assume $m_1 \geq m_2 \geq \dots \geq m_k$ w.l.o.g.; then it is suffice to apply dynamic programming to all subsets with size no more than m_1 .

Algorithm 3 The quantum divide-and-conquer algorithm for TSP.

Input: The weighted adjacency matrix $A = (\omega_{ij})_{n \times n}$. Let $n > m_1 \geq m_2 \geq \dots \geq m_k > 0$.

Output: The shortest Hamiltonian cycle and its cost.

- 1: Calculate $f(S_i, u_i, v_i)$ for all $|S_i| \leq m_1$ classically using (1).
 - 2: Prepare the uniform superposition state $|\psi\rangle$ encoding all elements of P , which we call the set partition state.
 - 3: Run quantum minimum finding over the components of the superposition state $|\psi\rangle$ to get the shortest Hamiltonian cycle, where the oracle can query classical data about $f(S_i, u_i, v_i)$ for $|S_i| \leq m_1$.
-

Algorithm 2 is a special case of **Algorithm 3** when $k = 8$ and $m_1 = \dots = m_4 = (1 - \alpha)n/4, m_5 = \dots = m_8 = \alpha n/4$. The query complexity of the classical part of **Algorithm 3** is

$$O^* \left(\sum_{i=1}^{m_1} \left(\binom{n}{1} + \binom{n}{2} + \dots + \binom{n}{m_1} \right) \right) = O^* \left(2^{nH(\frac{m_1}{n})} \right). \quad (9)$$

The query complexity of the quantum part is

$$O^* \left(\sqrt{\binom{n}{m_1} \binom{n-m_1}{m_2} \dots \binom{n - \sum_{i=1}^{k-2} m_i}{m_{k-1}}} \right) = O^* \left(\sqrt{\frac{n!}{\prod_{i=1}^k m_i!}} \right). \quad (10)$$

C. Optimal Query Complexity

Let $m_i = \alpha_i n$, $0 < \alpha_i < 1$, $1 \leq i \leq k-1$ and $m_k = (1 - \sum_{i=1}^{k-1} \alpha_i)n$. Then the query complexity of the classical part of **Algorithm 3** is

$$O^*(2^{nH(\alpha_1)}). \quad (11)$$

The query complexity of the quantum part is

$$\begin{aligned} & O^* \left(\sqrt{\binom{n}{\alpha_1 n} \binom{(1-\alpha_1)n}{\alpha_2 n} \cdots \binom{(1-\sum_{i=1}^{k-2} \alpha_i)n}{\alpha_{k-1} n}} \right) \\ & = O^* \left(2^{\frac{n}{2}(H(\alpha_1) + (1-\alpha_1)H(\frac{\alpha_2}{1-\alpha_1}) + \dots + (1-\sum_{i=1}^{k-2} \alpha_i)H(\frac{\alpha_{k-1}}{1-\sum_{i=1}^{k-2} \alpha_i}))} \right). \end{aligned} \quad (12)$$

Theorem 2. *The optimal query complexity of **Algorithm 3** is $O^*(1.865666\dots^n)$ and this optimal value is obtained when $k = 4$ and $\alpha_1 = \alpha_2 = \alpha_3 = 0.315742\dots$*

The proof of **Theorem 2** can be found in **Appendix C**. The trade-off governing the optimal k can be understood intuitively. The classical part precomputes the shortest paths within subsets of size at most $\alpha_1 n$, incurring a cost of $O^*(2^{nH(\alpha_1)})$. The quantum part searches over all ordered k -partitions with labels of origins and ends, incurring a cost of $O^*(\sqrt{n! / (\prod_{i=1}^k m_i!)})$. As k increases, each subset shrinks, so the classical pre-computation becomes cheaper. However, the number of possible ordered k -partitions grows rapidly with k , and the quantum search cost rises accordingly. At $k = 2$, there is no speedup because the classical cost is $O^*(2^n)$. At $k = 3, 4$, the tension between shrinking classical cost and growing quantum search space can reach an equilibrium, yielding the optimal exponents $0.918296\dots$ for $k = 3$ and $0.899691\dots$ for $k = 4$. Beyond $k = 4$, the growth in the number of ordered partitions outpaces the quadratic Grover speedup, and the overall complexity reverts to $\Omega(2^n)$.

Table I collects the query complexities of the algorithms discussed in this section. The corrected bound by the authors of [1] ($> 2^n$, specifically $2.225880\dots^n$ at the claimed optimal α) never surpasses Held–Karp; our optimal $k = 4$ framework achieves $1.865666\dots^n$, a genuine exponential speedup over the classical 2^n .

TABLE I: Summary of query complexities for general TSP. All bounds are expressed in the $O^*(\cdot)$ sense (ignoring polynomial factors).

| Algorithm | Query Complexity | Numerical Base (c^n) |
|----------------------------------------|-------------------------------------------------------|-------------------------------------|
| Held-Karp (classical DP) [21] | 2^n | 2^n |
| claimed in [1] | $2^{\frac{1}{2}(1+\frac{1}{2}+\frac{H(\alpha)}{4})n}$ | $1.727391\dots^n$ |
| correction of [1] (Theorem 1) | $2^{(1+\frac{H(\alpha)}{2})n}$ | $> 2^n$ |
| This work ($k = 4$, optimal) | $2^{0.899691\dots n}$ | $1.865666\dots^n$ |

We remark that while $k = 4$ is optimal, the numerical difference between $k = 3$ ($2^{0.918296\dots n} = 1.889881\dots^n$) and $k = 4$ ($1.865666\dots^n$) is modest, and $k = 3$ requires only three subsets, which simplifies the algorithm. Hence, for small to moderate n , $k = 3$ may be preferable in practice, and our Qiskit simulations (Section IV) indeed use $k = 3$.

III. IMPLEMENTATION OF THE ORACLE

A. Necessity of Structured State Preparation

In this section, we argue that our structured state preparation is necessary to keep each oracle query within polynomial time complexity. In other words, preparing the set partition state is indispensable for our TSP solver to achieve a genuine quantum advantage in total time complexity.

In our TSP solver, the oracle needs to query classical data. A straightforward approach is to use H -gates to create a uniform superposition state $\sum_{i=0}^{|P|-1} \frac{1}{\sqrt{|P|}} |i\rangle$, where P is the set of all ordered set partitions with labels; then construct a lookup table that maps each index i to an ordered set partition with labels, and query the corresponding classical data about the length of the route. However, this approach requires a bijection from sequential indices to ordered set partitions with labels, and the oracle must encode this bijection, which makes the oracle construction extremely challenging. To overcome this difficulty, we shift the burden of oracle construction to state preparation, i.e., utilizing the structured state to explicitly encode P . We generalize the method for preparing Dicke states to directly prepare the uniform superposition state that encodes ordered set partitions with labels, which we call the set partition state. Although this approach does not fully utilize the encoding space of quantum states, it bypasses the need to design and encode a bijection in the oracle by leveraging the structural nature of the set partition state.

In fact, the importance of the structured state preparation goes far beyond this. Considering using the bucket-brigade QRAM to implement the oracle, we show that the structured state preparation is indispensable to keep the total time complexity from exceeding that of the classical Held-Karp algorithm. (A brief introduction about the bucket-brigade QRAM can be found in **Appendix D**.) If we use trivial encoding method, i.e., utilizing the state $\sum_{i=0}^{|P|-1} \frac{1}{\sqrt{|P|}} |i\rangle |0\rangle^{\otimes M}$ (which can be prepared using H^{\otimes} gates); then the process of querying the QRAM is as follows:

Our TSP solver first pre-calculate the shortest paths for subsets S_i of size at most $\alpha_1 n$ by classical dynamic programming. Then we classically calculate the lengths of Hamiltonian cycles corresponding to all ordered set partitions with labels by querying the precomputed shortest paths $f(S_i, u_i, v_i)$ and the weights of connecting edges ω_{vu} , and subtract the threshold from these lengths to obtain the values of

$$f(S_A, 0, v_A) + \omega_{v_A u_B} + f(S_B, u_B, v_B) + \omega_{v_B u_C} + f(S_C, u_C, v_C) + \omega_{v_C u_D} + f(S_D, u_D, v_D) + \omega_{v_D 0} - C_T.$$

We save these values as a classical array $Arr = \{(i, v_i) : 0 \leq i \leq |P| - 1\}$ according to two's complement form. The elements of this array are assigned to the leaf nodes of the QRAM tree, and the binary strings corresponding to the paths from the root to these leaf nodes encode the indices of the array. In this way, the oracle can access classical data via QRAM. Therefore, we can obtain the state $\sum_{i=0}^{|P|-1} \frac{1}{\sqrt{|P|}} |i\rangle |v_i\rangle$ from the state $\sum_{i=0}^{|P|-1} \frac{1}{\sqrt{|P|}} |i\rangle |0\rangle^{\otimes M}$ through the QRAM query. Next, the oracle of our TSP solver applies Z -gate on the sign qubit and then resets the value register to its initial state $|0\rangle^{\otimes M}$ using the inverse of the QRAM query operation.

However, using the optimal parameters, we have $|P| = O^*(2^{2nH(\alpha_1)})$ (the quantum query complexity is $\sqrt{|P|}$). Hence, it requires the time complexity of $O^*(2^{2nH(\alpha_1)}) = O^*(1.865666\dots^{2n}) = O^*(3.480709\dots^n)$ to create the classical array $Arr = \{(i, v_i) : 0 \leq i \leq |P| - 1\}$ and assign its elements to the leaf nodes of the QRAM tree, meaning that the quantum advantage is swamped by classical overhead. We must compute values related to P in a quantum manner, and can only query the classical precomputed DP table of length $O^*(2^{nH(\alpha_1)})$, which force us to utilize the structured state to explicitly encode P .

B. Structured State

We can distinguish 4 subsets with labels A, B, C, D and use states 00, 01, 10, 11 to represent them respectively. To identify the origin u and the end v of the shortest path in a subset, we use four qubits to encode a vertex of the entire set S . A total of $4n$ qubits is required. Among the four qubits encoding each vertex, the first two qubits indicate which subset the vertex belongs to, and the last two qubits $|uv\rangle$ indicate the origin and end: If this vertex is the origin, then $u = 1$, $v = 0$. If this vertex is the end, then $u = 0$, $v = 1$. For other cases, $u = 0$, $v = 0$. Based on this encoding method, our set partition state is

$$\sum_{p \in P} \frac{1}{\sqrt{|P|}} |p\rangle = \sum_{p \in P} \frac{1}{\sqrt{|P|}} |**uv\rangle^{\otimes n}, \quad (13)$$

where P is the set of all ordered set partitions with labels, and $(**uv)$ represents the labels of subsets ($**$) and the origin ($u = 1$) or end ($v = 1$) for a single vertex. Every $p \in P$ corresponds to a Hamiltonian cycle.

Theorem 3. *The set partition state can be prepared with the gate complexity of $O(n^2)$ and the depth of $O(n)$ without ancillary qubits, and the algorithm is provided as **Algorithm 4** in **Appendix F**.*

The proof can be found in **Appendix F**, where readers need to first understand the details of the Dicke state preparation in **Appendix E**.

We also consider methods for preparing the uniform superposition states that encode Hamiltonian cycles and permutations of order n . Although our algorithm does not use these two superposition states, they are relevant to quantum search algorithm for solving TSP [14, 23]. (In the previous work [14], the authors utilized the superposition state of Hamiltonian cycles to index data combining a shortcut of QFT. In this work, we adopt the set partition state instead.) Actually, they are quantum counterparts of the classical random generation of cycles and permutations, which are Sattolo's algorithm [24, 25] and Fisher-Yates shuffle [26] respectively. Our quantum counterpart of Sattolo's algorithm is a small extension of the previous work [14]. Here, we improve the gate complexity from $O(n^{\frac{5}{2}})$ in [14] to $O(n^2 \log_2 n)$ by optimizing the order of adding vertices and execution of basic modules. Furthermore, we generalize it to the case of permutations. One can refer to the following theorem and its proof in **Appendix H** for details.

Theorem 4. *The superposition state of all Hamiltonian cycles of length n $\sum_{\sigma_n \in HC_n} \frac{1}{\sqrt{(n-1)!}} |\sigma_n\rangle$ can be prepared with the gate complexity of $O(n^2 \log_2 n)$ using $\lceil \log_2 n \rceil + 1$ ancillary qubits. Similarly, we can prepare the superposition state of all permutations of length n using the same resources.*

In the case of permutation, there is related work proposing the quantum Fisher-Yates shuffle [27], which shares the same underlying methods as our algorithm, i.e., quantizing classical random generation algorithms to prepare the superposition states.

C. Implementing Oracle with SBM

We first prepare the set partition state $\sum_{p \in P} \frac{1}{\sqrt{|P|}} |p\rangle |0\rangle^{\otimes 4M} = \sum_{p \in P} \frac{1}{\sqrt{|P|}} |**uv\rangle^{\otimes n} |0\rangle^{\otimes 4M}$ using **Algorithm 4**. Then we define Boolean functions $f_i : P \rightarrow \{0, 1\}^M$, where $f_i(p)$ is the binary value of the length of the shortest path in subset S_i , i.e., $f(S_i, u_i, v_i)$; and the corresponding sparse Boolean function selectors: $\text{select}(f_i) |p\rangle |z\rangle = |p\rangle |z \oplus f_i(p)\rangle$, where \oplus represents

bit-wise XOR. By Lemma 2 in [20], $\text{select}(f_i)$ can be realized with a quantum circuit with circuit depth $O(\log_2(4n|P|M)) = O(2nH(\alpha_1) + \log_2 M) = O(n)$ and $O(4n|P|M) = O^*(2^{2nH(\alpha_1)}) = O^*(3.480709\dots^n)$ ancillary qubits using only single- and two-qubit gates.

Denote $f(S_i, u_i, v_i)$ as f_i . We invoke the SBM four times ($i = A, B, C, D$) to transform the state $\sum_p \frac{1}{\sqrt{|P|}} |p\rangle |0\rangle |0\rangle |0\rangle |0\rangle$ into $\sum_p \frac{1}{\sqrt{|P|}} |p\rangle |f_A\rangle |f_B\rangle |f_C\rangle |f_D\rangle$. Then we use quantum adder to obtain $\sum_p \frac{1}{\sqrt{|P|}} |p\rangle |f_A + f_B + f_C + f_D\rangle |f_B\rangle |f_C\rangle |f_D\rangle$. The quantum adder is achievable; for example, one can refer to Appendix E.2. in [28]. Next, we load the weight of the edges connecting different subsets and threshold by applying QFT, controlled $U_G(\omega_{vu})$, controlled $U_G(-C_T)$ and QFT † , where the controlled $U_G(\theta)$ -gate is introduced in **Appendix G**. Now we obtain the state

$$\sum_p \frac{1}{\sqrt{|P|}} |p\rangle |f(S_A, u_A, v_A) + \omega_{v_A u_B} + f(S_B, u_B, v_B) + \omega_{v_B u_C} + f(S_C, u_C, v_C) + \omega_{v_C u_D} + f(S_D, u_D, v_D) + \omega_{v_D u_A} - C_T\rangle |f_B\rangle |f_C\rangle |f_D\rangle.$$

Mark the solutions with lengths lower than the threshold C_T by applying the Z -gate on the sign qubit of the second register. Finally, we free all value registers by applying the inverse operators.

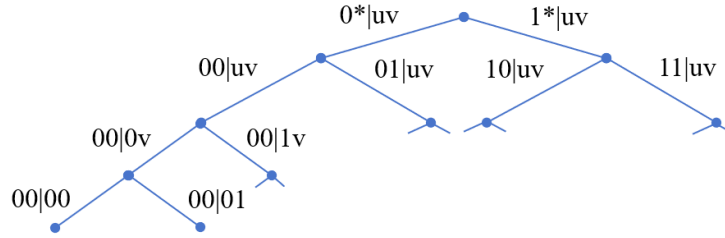


FIG. 1: Address transmission for one vertex (four qubits) in our encoding method. For the branches that mark the origins and ends, we only retain those corresponding to subset A.

We briefly explain how $\text{select}(f_i)$ accesses the shortest path data in the classical DP table based on the components $|p\rangle$ of the quantum state. The principle is similar to that of the bucket-brigade QRAM. The auxiliary qubits are organized into a tree-like logical structure, and the binary string encoded in each component serves as an address that determines an index path from the root node to a leaf node bit by bit. **Figure 1** illustrates how the 4-qubit encoding of each vertex determines the branching of the index path. When a qubit is in the state $|0\rangle$, the left branch is selected; otherwise, the right branch is selected. The first two qubits determine the subset label, while the last two qubits determine whether the current vertex is an origin or an end. Upon reaching a leaf node, the corresponding classical register is accessed. Every four qubits on the index path determine which subset the corresponding vertex belongs to, as well as whether it is an origin or an end. Therefore, the binary string of p directly indicates which four subsets, as well as their respective origins and ends, need to be retrieved, and the accessed registers can query the precomputed shortest path data $f(S_i, u_i, v_i)$ in parallel from the classical DP table directly.

Although the SBM requires exponential qubits and gate complexity, the circuit depth of the SBM is $O(n)$ under the optimal parameters ($k = 4$). Therefore, the oracle of our TSP solver can compute the lengths of the Hamiltonian cycles within polynomial time complexity. Assisted by the SBM, the total time complexity of our TSP solver is $O^*(1.865666\dots^n)$, which is superior to the best classical algorithm (Held-Karp).

IV. SIMULATION EXPERIMENTS

To demonstrate the performance of our TSP solver, we conducted simulation experiments on small instances using IBM’s Qiskit. Due to the qubit limitation of the simulator, we replace the SBM with the shortcut of QFT in the simulation experiments. **Figure 2** shows the framework of our TSP solver in the simulation experiments. We divide all qubits into the index register and the value register. *Ind*-module can prepare the set partition state in the index register. The controlled U_G -gate is a shortcut of QFT, which is introduced in **Appendix G**. The oracle queries the classical data based on the index register and calculates the lengths of the corresponding Hamiltonian cycles in the value register. The purple part is standard Grover’s diffusion operator $A(I - 2|0\rangle\langle 0|)A^\dagger$ with A replaced by *Ind*-module.

To reduce the additional resource consumption caused by redundant encoding of solutions, we stipulate that the salesman departs from vertex 0 and returns to vertex 0 at the end, i.e., 4-qubit encoding vertex 0 is fixed as $|0010\rangle$ and for the other vertices in subset A we set $|u\rangle = |0\rangle$. In this way, we eliminate n repetitions caused by different starting points, and the number of qubits occupied by *Ind*-module will also be reduced from $4n$ to $4(n - 1)$.

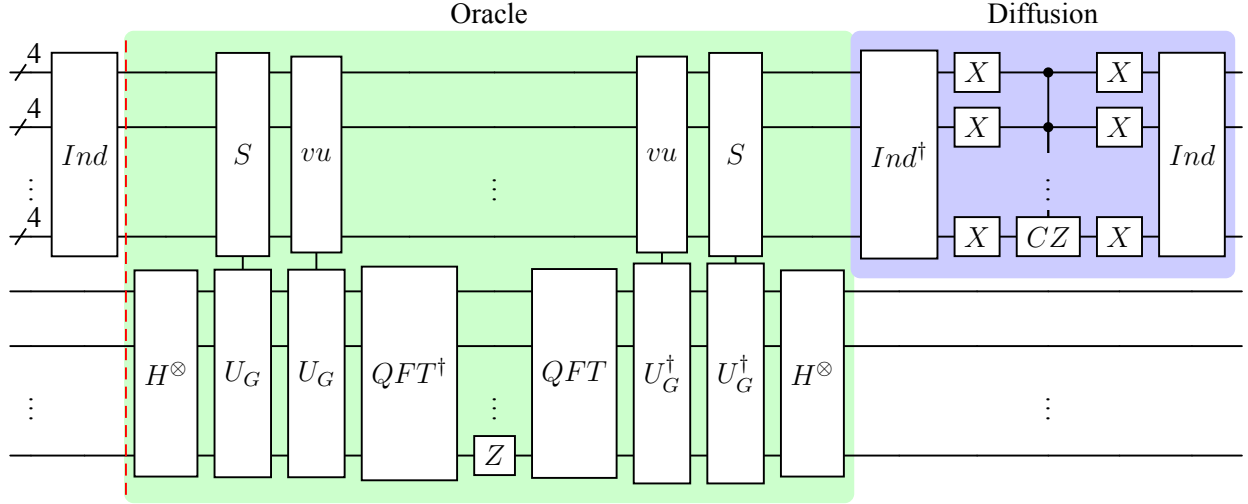


FIG. 2: The framework of our TSP solver, where the *Ind*-module represents the set partition state preparation algorithm and the controlled U_G -gate is introduced in **Appendix G**. The part to the right of the red dashed line is Grover search module, which will be executed many times to amplify the amplitude of the optimal solution.

V. RESULTS AND DISCUSSION

A. Results

Due to the memory limitation, we use the case of the ordered 3-partition for two graphs with node number $n = 6, 7$ and adopt shortcut of QFT to load the classical data. The same quantum circuit was executed for $shots = 1000$ times to obtain the statistical data of the components of the final quantum state. To simply verify the effectiveness of the algorithm, we set the threshold $C_T = w_{p^*} + 1$ where w_{p^*} is the length of the optimal solution. Of course, in practice the optimal solution is unknown at the beginning, and the threshold should be updated from an initial assumption value

by executing the quantum exponential searching [29, 30].

Table II shows our simulation results on IBM’s Qiskit, where “qubits” denotes the required number of qubits, “num” denotes the number of the optimal solutions, “iterations” denotes the optimal number of iterations, $x = \lceil \sqrt{\frac{(n-1)!}{(a-1)!b!c!\cdot\text{num}}} \rceil$ and “accuracy” is computed from the proportion of the optimal solutions in 1000 samples. For graph with $n = 6$, we take $a = 2$, $b = 2$, $c = 2$. For graph with $n = 7$, we take $a = 3$, $b = 2$, $c = 2$. The adjacency matrices of these two graphs are:

$$\mathbf{X}_6 = \begin{pmatrix} 0 & 1 & 3 & 2 & 2 & 1 \\ 1 & 0 & 1 & 3 & 1 & 2 \\ 3 & 1 & 0 & 3 & 2 & 3 \\ 2 & 3 & 3 & 0 & 1 & 1 \\ 2 & 1 & 2 & 1 & 0 & 3 \\ 1 & 2 & 3 & 1 & 3 & 0 \end{pmatrix}, \quad \mathbf{X}_7 = \begin{pmatrix} 0 & 1 & 3 & 2 & 2 & 1 & 1 \\ 1 & 0 & 1 & 3 & 1 & 2 & 1 \\ 3 & 1 & 0 & 3 & 2 & 3 & 1 \\ 2 & 3 & 3 & 0 & 1 & 1 & 1 \\ 2 & 1 & 2 & 1 & 0 & 3 & 1 \\ 1 & 2 & 3 & 1 & 3 & 0 & 1 \\ 1 & 1 & 1 & 1 & 1 & 1 & 0 \end{pmatrix}.$$

We also provide the bar charts in **Figure A10** in **Appendix I**.

TABLE II: Simulation Results

| | n | qubits | num | iterations | accuracy |
|-------|-----|--------|-----|------------|----------|
| X_6 | 6 | 25 | 2 | $x + 2$ | 98.9% |
| X_7 | 7 | 29 | 4 | $x + 5$ | 100% |

B. Discussion

In this work, we demonstrate that combining classical dynamic programming with quantum search can yield an achievable quantum advantage on the NP-hard traveling salesman problem. Our quantum divide-and-conquer strategy effectively provides a parameterized spectrum for this combination. **Algorithm 2** proposed in [1] corresponds to a specific case in this spectrum where $k = 8$ and $\alpha_1 = \dots = \alpha_4 = (1 - \alpha)/4$, $\alpha_5 = \dots = \alpha_8 = \alpha/4$, while the two extremes of the spectrum represent the purely classical Held-Karp and the purely quantum search algorithm, respectively. In particular, when $k = n$, the query complexity becomes $\sqrt{n!}$, which corresponds to directly searching over all permutations of order n for the optimal solution. If we let the salesman depart from vertex 0 and take $k = n - 1$, the query complexity will be $\sqrt{(n - 1)!}$, which corresponds to directly searching over all Hamiltonian cycles of order n for the optimal solution. To reduce the depth of each oracle query to the polynomial level, we resort to the SBM. This essentially trades an exponential number of qubits for polynomial circuit depth or time complexity.

In previous studies on quantum advantages for NP-hard combinatorial optimization problems, researchers focused only on improvements in query complexity. Our work, however, points out that the quantum advantage stems not only from the quadratic speedup of quantum search but also from structured quantum state preparation. The latter enables the parallel loading of classical data, eliminating the need to precompute, beyond the DP table, an additional long array that directly indexes the solutions to the problem. This avoids the extra classical overhead that would otherwise overwhelm the quantum advantage.

APPENDIX

A. The corrected complexity analysis of the algorithm for TSP in [1]

The number of solutions that the oracle of the quantum part in **Algorithm 2** must traverse is

$$N = O^* \left(\binom{n}{n/2} \binom{n/2}{n/4}^2 \binom{n/4}{\alpha n/4} \right), \quad (14)$$

not the $O^* \left(\binom{n}{n/2} \binom{n/2}{n/4} \binom{n/4}{\alpha n/4} \right)$ counted by the authors of [1]. Under Grover's algorithm [22], quantum minimum finding requires $O(\sqrt{N})$ queries, yielding the correct query complexity

$$O(\sqrt{N}) = O^* \left(2^n \binom{n/4}{\alpha n/4}^2 \right) = O^*(2^{n(1+H(\alpha)/2)}). \quad (15)$$

For the parameter $\alpha \approx 0.055362$ chosen by the authors of [1], this evaluates to $O^*(2.225880 \dots^n)$, which exceeds the classical Held-Karp bound of $O^*(2^n)$. In fact, the corrected quantum part satisfies $O(\sqrt{N}) > O^*(2^n)$ for any valid $\alpha > 0$, meaning the 8-subset scheme of [1] cannot surpass Held-Karp after the counting is corrected.

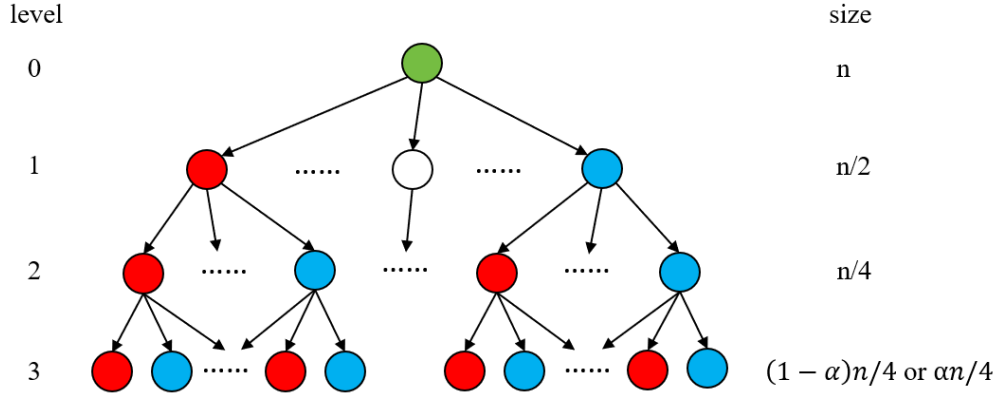


FIG. A1: Recursive tree of **Algorithm 2**.

Proof. In quantum minimum finding [29, 30], the oracle is required to mark solutions with lengths less than the current threshold, and the query complexity is $O(\sqrt{N})$ where N is the number of feasible solutions. **Figure A1** shows the recursive tree of **Algorithm 2**. The number of its leaf nodes is $\binom{n}{n/2} \binom{n/2}{n/4} \binom{n/4}{\alpha n/4}$, which is the number that the authors of [1] used to take the square root.

In **Algorithm 2**, step 2 must be executed as a single coherent quantum search, which requires that the oracle of quantum minimum finding can concatenate all possible paths according to the recursive tree before marking the feasible solutions. To determine a feasible solution, oracle has to trace the entire tree, rather than simply going from the root to a single leaf:

We select a subset of size $n/2$ from the entire set (the green root node at level 0 in **Figure A1**), and there are $\binom{n}{n/2}$ ways to do so. Let the red node at level 1 represent the selected subset, and its complement set be the blue node. Then, we select subsets of size $n/4$ from these two subsets (represented by the red and blue nodes at level 1) respectively, and there are $\binom{n/2}{n/4}^2$ ways to do so.

The authors of [1] only considered the number of ways of selecting from one subset (represented by the red node at level 1), ignoring the blue node! Similarly, we select subsets of size $\alpha n/4$ from four subsets at level 2, and there are $\binom{n/4}{\alpha n/4}^4$ ways to do so. Now we can construct a solution by concatenating the shortest paths of eight subsets at level 3. (We ignore the selection of the origin and end of the shortest path because this only increases a polynomial factor.) Therefore, there are $O^*\left(\binom{n}{n/2} \binom{n/2}{n/4}^2 \binom{n/4}{\alpha n/4}^4\right)$ solutions in total and each solution corresponds to an ordered partition of the entire set into 8 subsets with sizes of $\alpha n/4$ and $(1-\alpha)n/4$. Taking the square root and applying (6) yield the query complexity $O^*\left(2^n \binom{n/4}{\alpha n/4}^2\right) = O^*\left(2^{n(1+H(\alpha)/2)}\right)$. Substituting the parameter $\alpha \approx 0.055362$ from [1] gives the numerical value $O^*(2.225880\dots^n)$, which is strictly worse than the classical Held-Karp bound of $O^*(2^n)$. In fact, since $H(\alpha) \geq 0$, the corrected query complexity $O^*(2^{n(1+H(\alpha)/2)})$ cannot fall below $O^*(2^n)$ for any valid α , confirming that the 8-subset scheme never surpasses Held-Karp. \square

B. Divide-and-conquer

Let L_i denote the shortest path from u_i to v_i that passes through all vertices in S_i exactly once. Concatenate these paths into a cycle by adding edges $v_1u_2, v_2u_3, \dots, v_{k-1}u_k, v_ku_1$. Let all these cycles formed by all possible ordered k -partitions with sizes m_1, m_2, \dots, m_k and all possible selections of u_i, v_i for fixed S_i constitute a set P , then the shortest Hamiltonian cycle belongs to P .

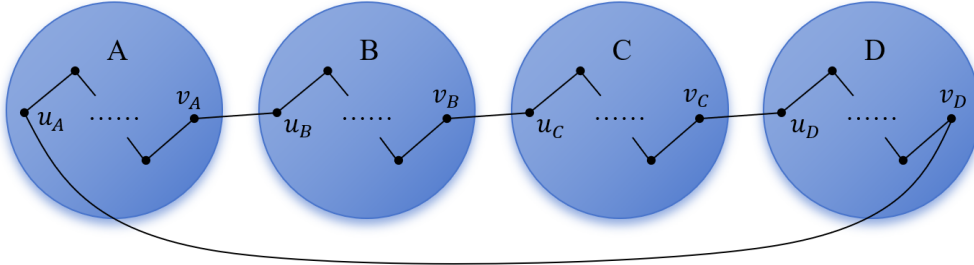


FIG. A2: Example of ordered 4-partition.

Proof. **Figure A2** shows an example of ordered 4-partition. Let the shortest Hamiltonian cycle be $w_1 \rightarrow w_2 \rightarrow \dots \rightarrow w_n \rightarrow w_1$. We can start from w_1 and select m_1, \dots, m_k vertices sequentially along the circle to form subsets S_1, \dots, S_k . Assume the origin and end of the cycle in S_i are u_i and v_i respectively. Then, the part of the cycle in S_i must be the shortest path from u_i to v_i that passes through all vertices exactly once in S_i . Otherwise, we can replace this path with the shortest path to obtain a shorter Hamiltonian cycle, leading to a contradiction. Therefore, the shortest Hamiltonian cycle belongs to P . \square

C. The optimal query complexity

Let $f(\alpha_1) = H(\alpha_1)$ and $g_k(\vec{\alpha}) = \frac{1}{2}(H(\alpha_1) + (1-\alpha_1)H(\frac{\alpha_2}{1-\alpha_1}) + \dots + (1 - \sum_{i=1}^{k-2} \alpha_i)H(\frac{\alpha_{k-1}}{1 - \sum_{i=1}^{k-2} \alpha_i}))$ denote the exponential parts of the classical and quantum complexities, respectively.

The optimal query complexity of **Algorithm 3** is $O^*(1.865666\dots^n)$ and this optimal value is obtained when $k = 4$ and $\alpha_1 = \alpha_2 = \alpha_3 = 0.315742\dots$

Proof. First, we show that $g_k(\vec{\alpha}) = -\frac{1}{2}[\sum_{i=1}^{k-1} \alpha_i \log_2 \alpha_i + (1 - \sum_{i=1}^{k-1} \alpha_i) \log_2(1 - \sum_{i=1}^{k-1} \alpha_i)]$. When $k = 2$, $g_2(\alpha_1) = \frac{1}{2}H(\alpha_1) = -\frac{1}{2}[\alpha_1 \log_2 \alpha_1 + (1 - \alpha_1) \log_2(1 - \alpha_1)]$. Assume the proposition holds for $k = t - 1$. Then, for $k = t$ we have:

$$\begin{aligned}
g_t(\vec{\alpha}) &= g_{t-1}(\vec{\alpha}) + \frac{1}{2}(1 - \sum_{i=1}^{t-2} \alpha_i)H\left(\frac{\alpha_{t-1}}{1 - \sum_{i=1}^{t-2} \alpha_i}\right) \\
&= -\frac{1}{2}\left[\sum_{i=1}^{t-2} \alpha_i \log_2 \alpha_i + (1 - \sum_{i=1}^{t-2} \alpha_i) \log_2(1 - \sum_{i=1}^{t-2} \alpha_i)\right] \\
&\quad - \frac{1}{2}(1 - \sum_{i=1}^{t-2} \alpha_i)\left(\frac{\alpha_{t-1}}{1 - \sum_{i=1}^{t-2} \alpha_i} \log_2 \frac{\alpha_{t-1}}{1 - \sum_{i=1}^{t-2} \alpha_i} + \frac{1 - \sum_{i=1}^{t-1} \alpha_i}{1 - \sum_{i=1}^{t-2} \alpha_i} \log_2 \frac{1 - \sum_{i=1}^{t-1} \alpha_i}{1 - \sum_{i=1}^{t-2} \alpha_i}\right) \\
&= -\frac{1}{2}\left[\sum_{i=1}^{t-1} \alpha_i \log_2 \alpha_i + (1 - \sum_{i=1}^{t-1} \alpha_i) \log_2(1 - \sum_{i=1}^{t-1} \alpha_i)\right] \tag{16}
\end{aligned}$$

Hence, the proposition holds for any $k \geq 2$ by induction.

Next, we prove that $g_k(\vec{\alpha})$ is monotonically decreasing in each of its variables. By (16), the gradient of $g_k(\vec{\alpha})$ is

$$\begin{aligned}
\nabla g_k(\vec{\alpha}) &= \left[-\frac{1}{2 \ln 2}(\ln \alpha_i + 1 - \ln\left(1 - \sum_{i=1}^{k-1} \alpha_i\right) - 1)\right]_{i=1}^{k-1} \\
&= \left(-\frac{1}{2} \log_2 \frac{\alpha_i}{1 - \sum_{i=1}^{k-1} \alpha_i}\right)_{i=1}^{k-1}. \tag{17}
\end{aligned}$$

We have $1 > \alpha_1 \geq \dots \geq \alpha_{k-1} \geq 1 - \sum_{i=1}^{k-1} \alpha_i > 0$ for $n > m_1 \geq m_2 \geq \dots \geq m_k > 0$, meaning that $\frac{\alpha_i}{1 - \sum_{i=1}^{k-1} \alpha_i} \geq 1$. Hence, $\nabla g_k(\vec{\alpha}) \leq 0$. Fix α_1 , then $f(\alpha_1)$ becomes a constant, and $g_k(\vec{\alpha})$ obtains the minimum value when $\alpha_1 = \alpha_2 = \dots = \alpha_{k-1}$. The total query complexity is dominated by $\max\{f(\alpha_1), g_k(\vec{\alpha})\}$. Therefore, we let $\alpha_1 = \alpha_2 = \dots = \alpha_{k-1}$ and denote $g_k^*(\alpha_1) = g_k(\vec{\alpha})|_{\alpha_1 = \dots = \alpha_{k-1}} = -\frac{1}{2}[(k-1)\alpha_1 \log_2 \alpha_1 + (1 - (k-1)\alpha_1) \log_2(1 - (k-1)\alpha_1)]$, then we only need to consider $\max\{f(\alpha_1), g_k^*(\alpha_1)\}$.

Finally, we calculate the optimal query complexity. Since $1 > \alpha_1 \geq \dots \geq \alpha_{k-1} \geq 1 - \sum_{i=1}^{k-1} \alpha_i > 0$, we have $\frac{1}{k} \leq \alpha_1 < \frac{1}{k-1}$. For $k = 2$, $f(\frac{1}{2}) = H(\frac{1}{2}) = 1$, meaning that the complexity can not be better than **Algorithm 1**. For $k \geq 3$, we have $\frac{1}{k-1} \leq \frac{1}{2}$, and $f(\alpha_1)$ is monotonically increasing in $[\frac{1}{k}, \frac{1}{k-1}]$.

$$\begin{aligned}
\nabla g_k^*(\alpha_1) &= -\frac{1}{2 \ln 2}[(k-1)(\ln \alpha_1 + 1) - (k-1) \ln(1 - (k-1)\alpha_1) - (k-1)] \\
&= \frac{k-1}{2} \log_2 \frac{1 - (k-1)\alpha_1}{\alpha_1} \tag{18}
\end{aligned}$$

Since $\frac{1-(k-1)\alpha_1}{\alpha_1} \in (0, 1]$, we know $g_k^*(\alpha_1)$ is monotonically decreasing in $[\frac{1}{k}, \frac{1}{k-1}]$. For $k > 4$, we have $f(\alpha_1) < f(\frac{1}{k-1})$ and $g_k^*(\alpha_1) > g_k^*(\frac{1}{k-1}) = -\frac{1}{2} \log_2 \frac{1}{k-1}$. Let $\frac{1}{k-1} \leq \frac{1}{4}$, then $g_k^*(\frac{1}{k-1}) = -\frac{1}{2} \log_2 \frac{1}{k-1} \geq -\frac{1}{2} \log_2 \frac{1}{4} = 1$, meaning that the complexity can not be better than **Algorithm 1**. For $k = 3, 4$, we know the complexity reaches optimal value when $f(\alpha_1) = g_k^*(\alpha_1)$ according to

the monotonicity of these two functions. Numerical calculation shows that the optimal values are $f(0.333333\dots) = g_3^*(0.333333\dots) = 0.918296\dots$ for $k = 3$ and $f(0.315742\dots) = g_4^*(0.315742\dots) = 0.899691\dots$ for $k = 4$.

Therefore, the optimal query complexity of **Algorithm 3** is $O^*(2^{0.899691\dots n}) = O^*(1.865666\dots^n)$. \square

When $k > 4$, the quantum divide-and-conquer can no longer beat **Algorithm 1**, because the quadratic speedup fails to surpass the exponential growth of the number of ordered partitions.

D. The bucket-brigade QRAM

The bucket-brigade QRAM architecture has been realized on the superconducting quantum processor for small models [31]. **Figure A3** shows the principle of the bucket-brigade QRAM loading 8 data items. The address bits within the green box are sequentially fed into the QRAM. At each step, a branch is selected based on whether the current bit is 0 or 1, while the subsequent address bits are then passed downward and stored in the green address register. Upon reaching a leaf node, the classical data item is loaded into the blue data register via quantum gates. The data is then either transmitted back along the reverse path of the address traversal or transferred to the target value register d via quantum teleportation. The transmission of address bits and data is implemented using the controlled-SWAP network. For specific details, please refer to [31].

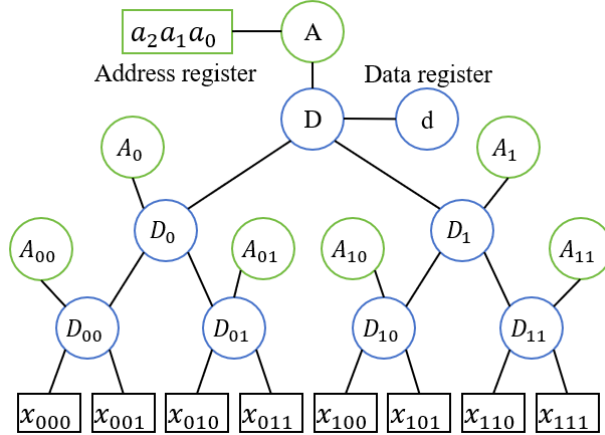


FIG. A3: Schematic diagram of the bucket-brigade QRAM loading 8 data items.

E. Dicke state preparation

The Dicke state [32], defined as the uniform superposition of all n -qubit states $|x\rangle$ with Hamming weight $w(x) = k$, i.e.,

$$|D_k^n\rangle = \sum_{x \in \{0,1\}^n, w(x)=k} \frac{1}{\sqrt{\binom{n}{k}}} |x\rangle, \quad (19)$$

can be used to index the subsets of the same size. Bartschi et al. [33] provided a deterministic method to efficiently prepare the Dicke state without any ancillary qubits, which requires $O(kn)$

quantum gates and a depth of $O(n)$. This method is based on the recursive formula

$$|D_k^n\rangle = \sqrt{\frac{n-k}{n}} |D_k^{n-1}\rangle |0\rangle + \sqrt{\frac{k}{n}} |D_{k-1}^{n-1}\rangle |1\rangle, \quad (20)$$

which starts from the initial state $|0\rangle^{\otimes(n-k)} |1\rangle^{\otimes k}$ and can be achieved by applying appropriate RY -gate. The quantum circuits for preparing Dicke states consist of two basic structures, shown in **Figure A4**.

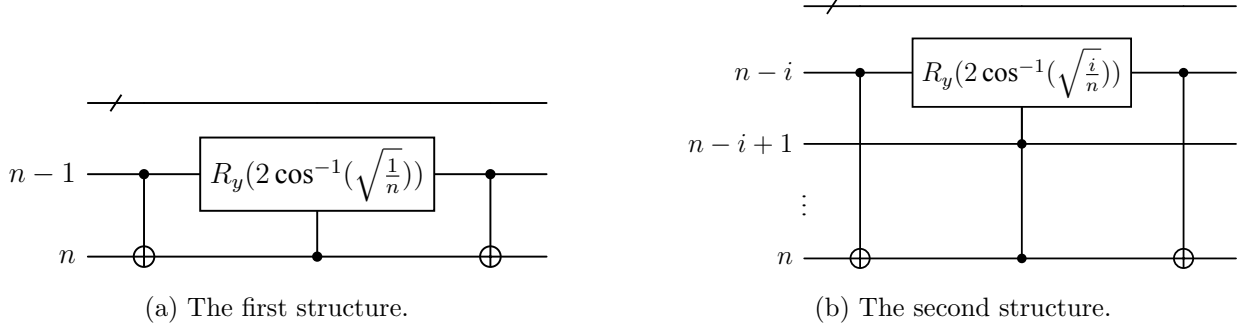


FIG. A4: Basic structures of the quantum circuits for preparing Dicke states.

Figure A5 provides a quantum circuit to prepare $|D_2^4\rangle$, in which the $RY(2 \cos^{-1} \sqrt{\frac{i}{m}})$ gate can transform the state $|0\rangle$ into the state $\sqrt{\frac{i}{m}} |0\rangle + \sqrt{\frac{m-i}{m}} |1\rangle$ and there are three modules with $m = 4, 3, 2$. In each module, the circuit scans upward from the current highest-order qubit (the m -th qubit counting from the top). Upon locating the first 0, a RY -gate is applied to generate two branches. For the branch where the qubit becomes $|1\rangle$, the corresponding $|1\rangle$ at the current highest-order qubit is flipped. As shown in **Figure A6**, the three layers of the binary tree (from left to right) correspond to the actions of the three modules. The underlined digits indicate the corresponding qubits that will not be modified in subsequent operations, and the digit immediately preceding an underlined digit represents the current highest-order qubit. The leaf nodes of the tree represent 6 components of $|D_2^4\rangle$.

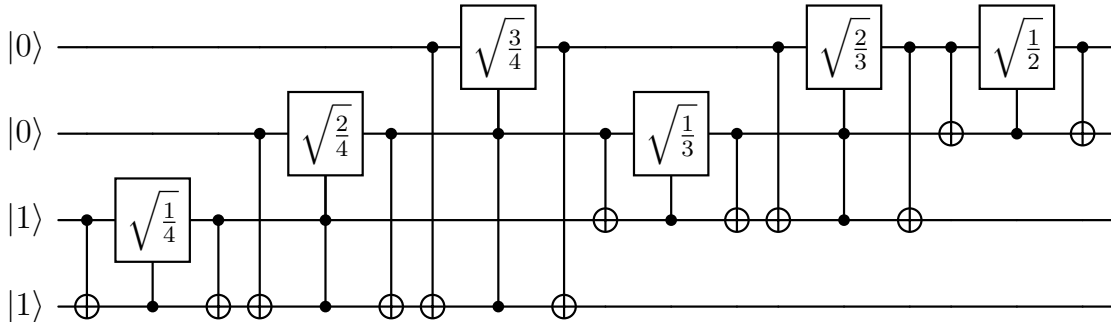


FIG. A5: Quantum circuit for preparing Dicke state of 4 qubits.

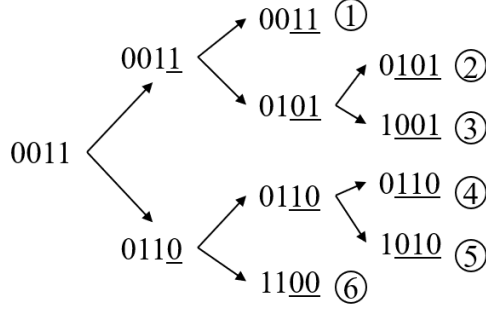


FIG. A6: The binary tree produced in preparing $|D_2^4\rangle$.

The Dicke state can be used to design quantum algorithms for some combinatorial optimization problems, such as k -vertex cover problem [18]. By the view of binary tree, we will generalize the Dicke state preparation method to the set partition state.

F. Set partition state preparation

The set partition state

$$\sum_{p \in P} \frac{1}{\sqrt{|P|}} |p\rangle = \sum_{p \in P} \frac{1}{\sqrt{|P|}} |**uv\rangle^{\otimes n}$$

can be prepared with the gate complexity of $O(n^2)$ and the depth of $O(n)$ without ancillary qubits. The preparation algorithm is provided as **Algorithm 4**:

Algorithm 4 The set partition state preparation algorithm for $k = 4$. We illustrate each step according to the column configuration of vertices (4 columns of qubits), as shown in **Figure A7**.

Input: Sizes of subsets a, b, c, d , where $a + b + c + d = n$. The initial state $|0\rangle^{\otimes 4n}$.

Output: The uniform superposition state of all ordered set partitions with labels: $\sum_{p \in P} \frac{1}{\sqrt{|P|}} |**uv\rangle^{\otimes n}$, where every 4-qubit encodes one vertex.

- 1: Apply X -gates to the first three columns of qubits to initialize them such that the first column of qubits is set to $|0\rangle^{\otimes(a+b)} |1\rangle^{\otimes(c+d)}$, the second column of qubits is set to $|0\rangle^{\otimes a} |1\rangle^{\otimes b} |0\rangle^{\otimes c} |1\rangle^{\otimes d}$, and the third column of qubits is set to $|0\rangle^{\otimes(a-2)} |1\rangle^{\otimes 2} |0\rangle^{\otimes(b-2)} |1\rangle^{\otimes 2} |0\rangle^{\otimes(c-2)} |1\rangle^{\otimes 2} |0\rangle^{\otimes(d-2)} |1\rangle^{\otimes 2}$.
 - 2: Apply the Dicke state preparation algorithms of $D_2^a, D_2^b, D_2^c, D_2^d$ to the third column of qubits for 4 subsets, respectively.
 - 3: Apply the basic modules in **Figure A8** to all possible $\binom{x}{2}$ two-qubit positions for 4 subsets, respectively, where $x = a, b, c, d$.
 - 4: Apply the Dicke state D_b^{a+b} preparation algorithm with basic modified structures such as example in **Figure A9** to the first $4(a+b)$ qubits, where the RY -gates act on the second column of qubits.
 - 5: Apply the Dicke state D_d^{c+d} preparation algorithm with basic modified structures such as example in **Figure A9** to the last $4(c+d)$ qubits, where the RY -gates act on the second column of qubits.
 - 6: Apply the Dicke state D_{c+d}^n preparation algorithm with basic modified structures such as example in **Figure A9** to all $4n$ qubits, where the RY -gates act on the first column of qubits.
-

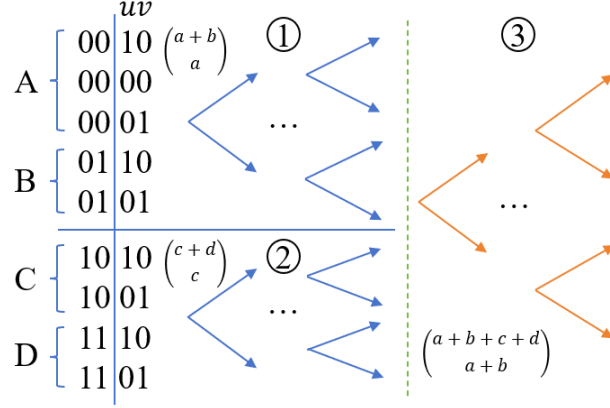


FIG. A7: The binary tree produced in preparing an ordered 4-partition state with size of 3, 2, 2, 2. A total of 36 qubits is used, where 4 qubits for each vertex, the first and second columns of qubits encode labels of subsets, and the third and fourth columns of qubits indicate the origin and end.

Proof. We can distinguish 4 subsets with labels A, B, C, D and use states 00, 01, 10, 11 to represent them respectively. To identify the origin u and the end v of the shortest path in a subset, we use four qubits to encode a vertex of the entire set S . A total of $4n$ qubits is required. Among the four qubits encoding each vertex, the first two qubits indicate which subset the vertex belongs to, and the last two qubits $|uv\rangle$ indicate the origin and end: If this vertex is the origin, then $u = 1$, $v = 0$. If this vertex is the end, then $u = 0$, $v = 1$. For other cases, $u = 0$, $v = 0$.

The step 1 of **Algorithm 4** creates the initial state for the Dicke state preparation algorithms. The step 2 and 3 of **Algorithm 4** encode the information of the origins and the ends. We apply the Dicke state preparation algorithms four times on the third column of qubits for subsets A, B, C, D respectively to get the state $|D_2^a\rangle |D_2^b\rangle |D_2^c\rangle |D_2^d\rangle$. Because one vertex can be either the origin or the end, we need to symmetrically allocate one of two $|1\rangle$ in each component of $|D_2^x\rangle$ to the fourth column of qubits. It can be done by applying the basic module in **Figure A8** in the step 3 of **Algorithm 4**.

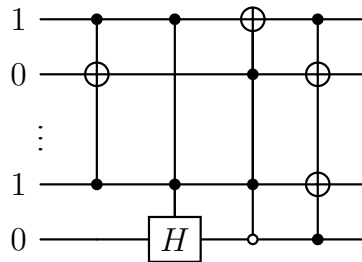


FIG. A8: Basic module to split the components in $|D_2^x\rangle$, where $x = a, b, c, d$.

The step 4-6 of **Algorithm 4** encode the information of ordered set partitions. For the set composed of subsets A and B, the first column of qubits is in state $|0\rangle$ and the second column of qubits distinguishes the labels A and B. Therefore, we can prepare the Dicke state D_b^{a+b} over the second column of qubits, which is marked as stage 1 in **Figure A7**. Similarly, we can prepare the Dicke state D_d^{c+d} over the second column of qubits for subsets C and D, which is marked as stage 2 in **Figure A7**; and prepare the Dicke state $D_{c+d}^{a+b+c+d}$ over the first column of qubits for all four subsets, which is marked as stage 3. When we apply the quantum gates of the Dicke state

preparation circuit to a certain qubit, we must ensure that the other qubits encoding the same vertex are correspondingly acted upon. Hence, we need to modify the basic structures in **Figure A4**. The modified structures are provided in **Figure A9**, where we use controlled SWAP-gates to ensure that the information of other qubits follows the qubit acted upon by R_Y -gates.

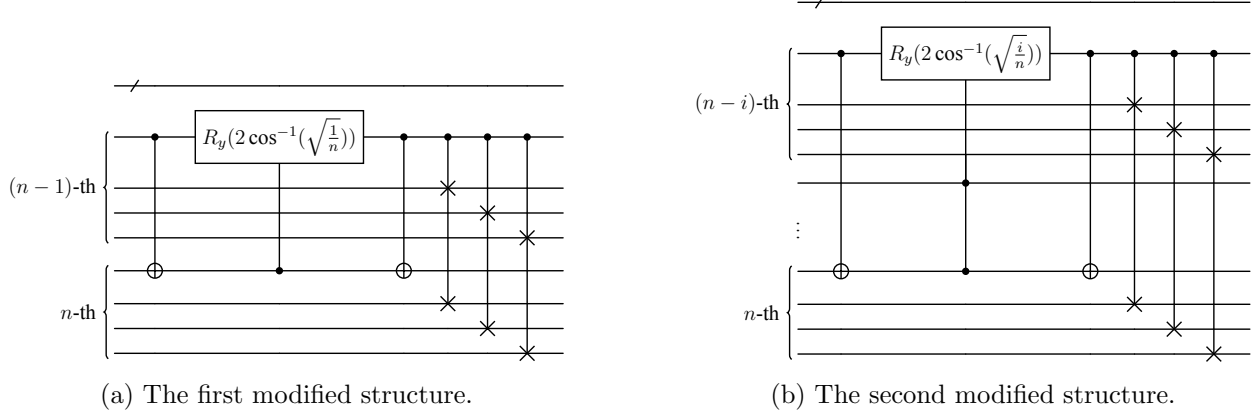


FIG. A9: Basic modified structures of the quantum circuits for preparing the set partition states, where a vertex is encoded by 4 qubits and in this figure the set composed of the first qubit of every vertex is acted upon by the R_Y -gates in the Dicke state preparation circuit.

Finally, we demonstrate that we can obtain the set partition state correctly because the process encoding ordered set partitions does not destroy the information about origins and ends:

Figure A7 shows similar binary trees as **Figure A6**. After the stage 1 finished, there is a binary tree with $\binom{a+b}{a}$ leaf nodes. For states of all qubits are organized by tensor product, every leaf nodes will connect a new tree with $\binom{c+d}{c}$ leaf nodes after the stage 2 finished. We obtain a tree with $\binom{a+b}{a} \binom{c+d}{c}$ leaf nodes. After the stage 3 finished, every leaf node of this tree connect a new tree with $\binom{a+b+c+d}{a+b}$ leaf nodes again. Finally, we obtain a tree with $\binom{a+b}{a} \binom{c+d}{c} \binom{a+b+c+d}{a+b} = \frac{(a+b+c+d)!}{a!b!c!d!}$ leaf nodes. Each path from the root to a leaf in this tree defines a mapping that sends the initial state to a particular component of the final state. This mapping, composed of a series of swap and identity, is a permutation. For permutation is bijective, we know that the process encoding ordered set partitions does not destroy the information about origins and ends: All the $2^4 \binom{a}{2} \binom{b}{2} \binom{c}{2} \binom{d}{2}$ marked u, v pairs are simply permuted. Hence, we get $2^4 \binom{a}{2} \binom{b}{2} \binom{c}{2} \binom{d}{2} \frac{(a+b+c+d)!}{a!b!c!d!}$ components corresponding to all possible origins u , ends v , and ordered 4-partitions with sizes of a, b, c, d .

The step 2 of **Algorithm 4** requires the gate complexity of $O(4 \cdot 2n) = O(n)$. The step 3 of **Algorithm 4** requires the gate complexity of $O(4 \binom{n}{2}) = O(n^2)$ and the depth of $O(n)$. The step 4-6 of **Algorithm 4** requires the gate complexity of $O(3n^2) = O(n^2)$ and the depth of $O(n)$. Therefore, our algorithm requires the gate complexity of $O(n^2)$ and the depth of $O(n)$ totally. \square

G. Shortcut of QFT

In the simulation experiment, we utilize a shortcut of the quantum Fourier transform (QFT) to calculate the data in value register under the control of the index register. Gilliam et al. [15] proposed this shortcut to address the constrained polynomial binary optimization (CPBO). We extend this idea to generally handle the value register through the index register.

Define the operator $U_G(\theta) = \bigotimes_{l=0}^{M-1} R(2^l\theta)$, one can verify

$$U_G(\theta)H^{\otimes M}|0\rangle^{\otimes M} = \frac{1}{\sqrt{2^M}} \sum_{j=0}^{2^M-1} \exp(ij\theta) |j\rangle_M, \quad (21)$$

which is very similar to

$$QFT|k\rangle = \frac{1}{\sqrt{2^M}} \sum_{j=0}^{2^M-1} \exp\left(\frac{2\pi i k j}{2^M}\right) |j\rangle_M, \quad 0 \leq k \leq 2^M - 1. \quad (22)$$

Hence, when θ is fixed, $U_G(\theta)$ can be regarded as a shortcut of QFT because there are no multi-qubit interactions in $U_G(\theta)$. Take $\theta = 2\pi k/2^M$ ($-2^{M-1} \leq k < 2^{M-1}$), combining (21) and (22) we have

$$QFT^\dagger U_G(\theta)H^{\otimes M}|0\rangle^{\otimes M} = |k \bmod 2^M\rangle. \quad (23)$$

For $-2^{M-1} \leq k < 0$ we have $|k \bmod 2^M\rangle = |k + 2^M \bmod 2^M\rangle$, meaning that the highest (left-most) digit is 1. Therefore, we can easily identify a negative number by examining its sign qubit (the highest digit). Although (23) can only encode the integer exactly, there are two methods in [15] to handle general real numbers, which are approximating real coefficients by fractions and encoding real coefficients as Fejér distributions, respectively. Now, we can encode data into θ and operate the value register using $U_G(\theta)$ controlled by index register. Particularly, $U_G(\theta)$ has the property of

$$U_G(\theta_1)U_G(\theta_2) = U_G(\theta_1 + \theta_2), \quad (24)$$

which facilitates the addition of two values. To circumvent the hardware challenges associated with implementing quantum gates that require exponentially small parameters, we usually set $M = c\lceil \log_2 n \rceil$ so that $2^M = O(n^c)$. Increasing the value of the constant c can improve encoding accuracy.

In **Figure 2**, U_G operators controlled by S -module are divided into four groups because we want to utilize the localized matching technology to match the subsets with label A, B, C, D separately. For example, we use $2\binom{b}{2}\binom{n-1}{b}$ controlled $U_G(f(S_B, u_B, v_B))$ operators with $4b$ controlling qubits taking all possible combinations in $4(n-1)$ qubits. (Every 4 qubits are bound together to encode a vertex.) After we applied all $\binom{a}{1}\binom{n-1}{a} + 2\binom{b}{2}\binom{n-1}{b} + 2\binom{c}{2}\binom{n-1}{c} + 2\binom{d}{2}\binom{n-1}{d}$ controlled U_G operators, we obtain

$$QFT|f(S_A, 0, v_A) + f(S_B, u_B, v_B) + f(S_C, u_C, v_C) + f(S_D, u_D, v_D)\rangle \quad (25)$$

in the value register. Then we utilize U_G operators controlled by vu -module to match the edge connections between subsets with different labels. For example, we use $2\binom{n-1}{2}$ controlled $U_G(\omega_{v_A u_B})$ with controlling qubits matching all possible $|0001\rangle, |0110\rangle$ pairs located in $4(n-1)$ qubits. After we applied these $\binom{n-1}{1} + 3 \cdot 2\binom{n-1}{2}$ controlled U_G operators, we obtain

$$\begin{aligned} & QFT|f(S_A, 0, v_A) + \omega_{v_A u_B} + f(S_B, u_B, v_B) + \omega_{v_B u_C} + f(S_C, u_C, v_C) + \omega_{v_C u_D} \\ & \quad + f(S_D, u_D, v_D) + \omega_{v_D 0}\rangle \\ = & QFT|\text{length of a certain Hamiltonian cycle}\rangle \end{aligned} \quad (26)$$

in the value register. Finally, $U_G(-C_T)$ (which is not drawn in **Figure 2**) and QFT^\dagger act on the

value register. Now we can use Z -gate acting on the sign qubit to mark a solution with length lower than threshold C_T . By applying the inverses of the above operators (except Z -gate) we can uncompute the value register.

Through quantum exponential searching [29, 30], we can find the optimal solution by iteratively updating the threshold.

H. State preparation for Hamiltonian cycle and permutation

The following two straightforward lemmas enable the iterative generation of Hamiltonian cycles and permutations.

Lemma 2. *Given a new vertex $v \notin \{1, \dots, k-1\}$, a Hamiltonian cycle of length $k-1$ denoted by $\sigma_{k-1} = [\sigma_{k-1}(1), \sigma_{k-1}(2), \dots, \sigma_{k-1}(k-1)]$ (as a permutation). We can generate $k-1$ different Hamiltonian cycles of length k where $1 \leq i \leq k-1$:*

$$\sigma_k = \begin{pmatrix} 1 & 2 & \dots & i & \dots & k-1 & v \\ \sigma_{k-1}(1) & \sigma_{k-1}(2) & \dots & v & \dots & \sigma_{k-1}(k-1) & \sigma_{k-1}(i) \end{pmatrix}.$$

If we already have all Hamiltonian cycles of length $k-1$, then we can obtain all Hamiltonian cycles of length k using the above method.

Lemma 3. *Given a new vertex $v \notin \{1, \dots, k-1\}$, a permutation of length $k-1$ denoted by $\sigma_{k-1} = [\sigma_{k-1}(1), \sigma_{k-1}(2), \dots, \sigma_{k-1}(k-1)]$. we can generate k different permutations of length k where $1 \leq i \leq k-1$:*

$$\sigma_k = \begin{pmatrix} 1 & \dots & i & \dots & k-1 & v \\ \sigma_{k-1}(1) & \dots & v & \dots & \sigma_{k-1}(k-1) & \sigma_{k-1}(i) \end{pmatrix} \text{ and } \sigma_k = \begin{pmatrix} 1 & \dots & k-1 & v \\ \sigma_{k-1}(1) & \dots & \sigma_{k-1}(k-1) & v \end{pmatrix}.$$

If we already have all permutations of length $k-1$, then we can obtain all permutations of length k through the above method.

We usually take v as k , meaning that we add new vertices in ascending order to iteratively generate Hamiltonian cycles and permutations. The iterative processes in **Lemma 2** and **Lemma 3** can be quantized to prepare the uniform superposition states that encode Hamiltonian cycles and permutations of order n .

Before proving **Theorem 4**, we also need the following lemma.

Lemma 4. *Let $m = \lceil \log_2 n \rceil$, $x = x_{m-1}x_{m-2} \dots x_0$ and $y = y_{m-1}y_{m-2} \dots y_0$ be binary representations of positive integers x , y . Define the following binary operation:*

$$x \oplus_0 y = \begin{cases} 0, & \text{if } x = y \\ x, & \text{if } x \neq y \end{cases}. \quad (27)$$

We can borrow $m+1$ auxiliary qubits to transform the state $\sum_{x,y} c_{xy} |x\rangle_1 |y\rangle_2 |0\rangle_a |0\rangle_b$ into the state $\sum_{x,y} c_{xy} |x \oplus_0 y\rangle |y\rangle |0\rangle_a |0\rangle_b$ with the gate complexity of $O(m)$, where $|0\rangle_a$ represents m ancillary qubits and $|0\rangle_b$ represents 1 extra ancillary qubits, $\sum_{x,y} |c_{xy}|^2 = 1$.

Proof. For convenience, we omit the summation about c_{xy} and consider XOR operation \oplus and

addition $+$ in \mathbb{F}_2 as equivalent. Perform the following operations (28, 30-31) in sequence:

$$\prod_{i=0}^{m-1} C_{1i} C_{2i} X_{ai} \prod_{j=0}^{m-1} X_{aj} |x\rangle_1 |y\rangle_2 |0\rangle_a |0\rangle_b = |x\rangle |y\rangle \otimes \left(\bigotimes_{i=0}^{m-1} |1 + x_i + y_i\rangle \right) |0\rangle_b, \quad (28)$$

where the subscript in the controlled X gate represents the position of the corresponding qubit. For example, $\bar{C}_1^m C_{2j} X_{aj}$ is a controlled X gate where anti-control qubits are m qubits in the first register, control qubit is the j -th qubit in the second register and the target qubit is the j -th qubit in the ancillary register $|0\rangle_a$. Define

$$\mathbf{1}_{x=y} \equiv \prod_{i=0}^{m-1} (1 + x_i + y_i) = \begin{cases} 1, & \text{if } x = y \\ 0, & \text{if } x \neq y \end{cases}. \quad (29)$$

$$\begin{aligned} & \prod_{i=0}^{m-1} C_{1i} C_{2i} X_{ai} \prod_{j=0}^{m-1} X_{aj} \cdot C_a^m X_b |x\rangle_1 |y\rangle_2 \left(\bigotimes_{k=0}^{m-1} |1 + x_k + y_k\rangle_a \right) |0\rangle_b \\ = & \prod_{i=0}^{m-1} C_{1i} C_{2i} X_{ai} \prod_{j=0}^{m-1} X_{aj} |x\rangle_1 |y\rangle_2 \left(\bigotimes_{k=0}^{m-1} |1 + x_k + y_k\rangle_a \right) |\mathbf{1}_{x=y}\rangle_b = |x\rangle |y\rangle |0\rangle_a |\mathbf{1}_{x=y}\rangle_b, \end{aligned} \quad (30)$$

$$\begin{aligned} & \bar{C}_1^m X_b \prod_{j=0}^{m-1} C_b C_{2j} X_{1j} |x\rangle_1 |y\rangle_2 |0\rangle_a |\mathbf{1}_{x=y}\rangle_b \\ = & \bar{C}_1^m X_b \left(\bigotimes_{j=0}^{m-1} |x_j \oplus y_j \cdot \mathbf{1}_{x=y}\rangle \right) |y\rangle |0\rangle_a |\mathbf{1}_{x=y}\rangle_b = \bar{C}_1^m X_b |x \oplus_0 y\rangle_1 |y\rangle_2 |0\rangle_a |\mathbf{1}_{x=y}\rangle_b \\ = & |x \oplus_0 y\rangle |y\rangle |0\rangle_a |\mathbf{1}_{x=y} \oplus \mathbf{1}_{x=y}\rangle = |x \oplus_0 y\rangle |y\rangle |0\rangle_a |0\rangle_b. \end{aligned} \quad (31)$$

Collecting all the above operations, this algorithm requires $2m$ X gates, $3m$ controlled X gates with 2 controlling qubits and 2 controlled X gates with m controlling qubits. By results about the decomposition of MCX gate [34], this algorithm is implementable with the gate complexity of $O(m)$. \square

Proof of **Theorem 4**:

Proof. Let $m = \lceil \log_2 n \rceil$. We need nm qubits to encode a Hamiltonian cycle σ_n of length n into $|\sigma_n\rangle = \bigotimes_{i=0}^{n-1} |\sigma_n(i)\rangle$. We prove the theorem by mathematical induction.

Beginning from $|0\rangle_a^{\otimes nm} |0\rangle_a^{\otimes (m+1)}$, where $|0\rangle_a^{\otimes (m+1)}$ represents ancillary qubits, we can obtain the state $|0\rangle_a^{\otimes m} |21\rangle |0\rangle_a^{\otimes (n-3)m} |0\rangle_a^{\otimes (m+1)}$ encoding $HC_2 = \{\sigma_2 = [2, 1]\}$ by applying some appropriate X gates. Suppose we have already prepared the state

$$|0\rangle_a^{\otimes m} \left(\sum_{\sigma_{k-1} \in HC_{k-1}} \frac{1}{\sqrt{(k-2)!}} \bigotimes_{j=1}^{k-1} |\sigma_{k-1}(j)\rangle \right) |0\rangle_a^{\otimes (n-k)m} |0\rangle_a^{\otimes (m+1)}. \quad (32)$$

Perform the following operations in sequence when $k < n$:

$$\begin{aligned}
U_1 & \left[|0\rangle^{\otimes m} \left(\sum_{\sigma_{k-1} \in HC_{k-1}} \frac{1}{\sqrt{(k-2)!}} \bigotimes_{j=1}^{k-1} |\sigma_{k-1}(j)\rangle \right) |0\rangle^{\otimes(n-k)m} |0\rangle_a^{\otimes(m+1)} \right] \\
& = |0\rangle^{\otimes m} \left(\sum_{\sigma_{k-1} \in HC_{k-1}} \frac{1}{\sqrt{(k-2)!}} \bigotimes_{j=1}^{k-1} |\sigma_{k-1}(j)\rangle \right) \otimes (G_k |0\rangle^{\otimes m}) \otimes |0\rangle^{\otimes(n-k-1)m} |0\rangle_a^{\otimes(m+1)} \quad (33)
\end{aligned}$$

$$= |0\rangle^{\otimes m} \left(\sum_{\sigma_{k-1} \in HC_{k-1}} \frac{1}{\sqrt{(k-2)!}} \bigotimes_{j=1}^{k-1} |\sigma_{k-1}(j)\rangle \right) \otimes \left(\sum_{i=1}^{k-1} \frac{1}{\sqrt{k-1}} |i\rangle \right) \otimes |0\rangle^{\otimes(n-k-1)m} |0\rangle_a^{\otimes(m+1)}. \quad (34)$$

In formula (33), G_k represents the Grover algorithm with zero theoretical failure rate [35]. By **Lemma 4**, we can realize the operation

$$\begin{aligned}
U_2 & \left[|0\rangle^{\otimes m} \left(\sum_{\sigma_{k-1} \in HC_{k-1}} \frac{1}{\sqrt{(k-2)!}} \bigotimes_{j=1}^{k-1} |\sigma_{k-1}(j)\rangle \right) \otimes \left(\sum_{i=1}^{k-1} \frac{1}{\sqrt{k-1}} |i\rangle \right) \otimes |0\rangle^{\otimes(n-k-1)m} |0\rangle_a^{\otimes(m+1)} \right] \\
& = |0\rangle^{\otimes m} \left(\sum_{\sigma_{k-1} \in HC_{k-1}} \sum_{i=1}^{k-1} \frac{1}{\sqrt{(k-1)!}} \left(\bigotimes_{j=1}^{k-1} |\sigma_{k-1}(j) \oplus_0 i\rangle \right) \otimes |i\rangle \right) |0\rangle^{\otimes(n-k-1)m} |0\rangle_a^{\otimes(m+1)}. \quad (35)
\end{aligned}$$

Isolate the following part from (35):

$$\sum_{\sigma_{k-1} \in HC_{k-1}} \sum_{i=1}^{k-1} \frac{1}{\sqrt{(k-1)!}} \left(\bigotimes_{j=1}^{k-1} |\sigma_{k-1}(j) \oplus_0 i\rangle \right) \otimes |i\rangle |0\rangle_a, \quad (36)$$

where $|0\rangle_a$ is the 0-th qubit in $|0\rangle_a^{\otimes(m+1)}$. Finally, we need to transform the state $|\sigma_{k-1}(j) \oplus_0 i\rangle$ into $|k\rangle$ when $\sigma_{k-1}(j) \oplus_0 i = 0$:

$$\begin{aligned}
& \prod_{j=1}^{k-1} C_j(k) X_a \prod_{j=1}^{k-1} C_a X_j(k) \prod_{j=1}^{k-1} \bar{C}_j^m X_a \sum_{\sigma_{k-1} \in HC_{k-1}} \sum_{i=1}^{k-1} \frac{1}{\sqrt{(k-1)!}} \left(\bigotimes_{j=1}^{k-1} |\sigma_{k-1}(j) \oplus_0 i\rangle_j \right) \otimes |i\rangle |0\rangle_a \\
& = \prod_{j=1}^{k-1} C_j(k) X_a \prod_{j=1}^{k-1} C_a X_j(k) \sum_{\sigma_{k-1} \in HC_{k-1}} \sum_{i=1}^{k-1} \frac{1}{\sqrt{(k-1)!}} \left(\bigotimes_{j=1}^{k-1} |\sigma_{k-1}(j) \oplus_0 i\rangle_j \right) \otimes |i\rangle |\mathbf{1}_{\sigma_{k-1}(j)=i}\rangle_a \\
& = \prod_{j=1}^{k-1} C_j(k) X_a \sum_{\sigma_{k-1} \in HC_{k-1}} \sum_{i=1}^{k-1} \frac{1}{\sqrt{(k-1)!}} \left(\bigotimes_{j=1}^{k-1} |\sigma_{k-1}(j) \oplus_0 i + k \cdot \mathbf{1}_{\sigma_{k-1}(j)=i}\rangle_j \right) \otimes |i\rangle |\mathbf{1}_{\sigma_{k-1}(j)=i}\rangle_a \\
& = \sum_{\sigma_{k-1} \in HC_{k-1}} \sum_{i=1}^{k-1} \frac{1}{\sqrt{(k-1)!}} \left(\bigotimes_{j=1}^{k-1} |\sigma_{k-1}(j) \oplus_0 i + k \cdot \mathbf{1}_{\sigma_{k-1}(j)=i}\rangle_j \right) \otimes |i\rangle |0\rangle_a, \quad (37)
\end{aligned}$$

where $\bar{C}_j^m X_a$ flips $|0\rangle_a$ when $|\sigma_{k-1}(j) \oplus_0 i\rangle_j = |0\rangle_j$, $C_a X_j(k)$ transforms the state $|0\rangle_j$ into $|k\rangle_j$ when the ancillary qubit is in the state $|1\rangle_a$, $C_j(k) X_a$ resets $|1\rangle_a$ to $|0\rangle_a$ by matching the binary representation of k encoded in control qubits $|*\rangle_j$. We can set $i = \sigma_{k-1}(t)$, $t \in \{1, \dots, k-1\}$ for σ_{k-1} is bijective. By **Lemma 2**, we have:

$$\begin{aligned}
& \sum_{\sigma_{k-1} \in HC_{k-1}} \sum_{i=1}^{k-1} \frac{1}{\sqrt{(k-1)!}} \left(\bigotimes_{j=1}^{k-1} |\sigma_{k-1}(j) \oplus_0 i + k \cdot \mathbf{1}_{\sigma_{k-1}(j)=i}\rangle_j \right) \otimes |i\rangle |0\rangle_a \\
= & \sum_{\sigma_{k-1} \in HC_{k-1}} \sum_{t=1}^{k-1} \frac{1}{\sqrt{(k-1)!}} \left(\bigotimes_{j=1}^{k-1} |\sigma_{k-1}(j) \oplus_0 \sigma_{k-1}(t) + k \cdot \mathbf{1}_{\sigma_{k-1}(j)=\sigma_{k-1}(t)}}\rangle_j \right) \otimes |\sigma_{k-1}(t)\rangle |0\rangle_a \\
= & \sum_{\sigma_{k-1} \in HC_{k-1}} \sum_{t=1}^{k-1} \frac{1}{\sqrt{(k-1)!}} \left(\bigotimes_{j=1}^{t-1} |\sigma_{k-1}(j)\rangle \right) |k\rangle \left(\bigotimes_{j=t+1}^{k-1} |\sigma_{k-1}(j)\rangle \right) |\sigma_{k-1}(t)\rangle |0\rangle_a \\
= & \sum_{\sigma_k \in HC_k} \frac{1}{\sqrt{(k-1)!}} |\sigma_k\rangle |0\rangle_a. \tag{38}
\end{aligned}$$

When we have obtained the state $|0\rangle^{\otimes m} \sum_{\sigma_{n-1} \in HC_{n-1}} \frac{1}{\sqrt{(n-2)!}} |\sigma_{n-1}\rangle |0\rangle_a^{\otimes(m+1)}$ by induction, we perform the last step (We don't consider 0 until the last step because **Lemma 4** requires $x \neq 0$):

$$\begin{aligned}
& U_1 \left[|0\rangle^{\otimes m} \left(\sum_{\sigma_{n-1} \in HC_{n-1}} \frac{1}{\sqrt{(n-2)!}} \bigotimes_{j=1}^{n-1} |\sigma_{n-1}(j)\rangle \right) |0\rangle_a^{\otimes(m+1)} \right] \\
& = (G_n |0\rangle^{\otimes m}) \otimes \left(\sum_{\sigma_{n-1} \in HC_{n-1}} \frac{1}{\sqrt{(n-2)!}} \bigotimes_{j=1}^{n-1} |\sigma_{n-1}(j)\rangle \right) |0\rangle_a^{\otimes(m+1)} \\
& = \left(\sum_{i=1}^{n-1} \frac{1}{\sqrt{n-1}} |i\rangle \right) \otimes \left(\sum_{\sigma_{n-1} \in HC_{n-1}} \frac{1}{\sqrt{(n-2)!}} \bigotimes_{j=1}^{n-1} |\sigma_{n-1}(j)\rangle \right) |0\rangle_a^{\otimes(m+1)}. \tag{39}
\end{aligned}$$

By **Lemma 4**, we can realize the operation

$$\begin{aligned}
& U_2 \left[\left(\sum_{i=1}^{n-1} \frac{1}{\sqrt{n-1}} |i\rangle \right) \otimes \left(\sum_{\sigma_{n-1} \in HC_{n-1}} \frac{1}{\sqrt{(n-2)!}} \bigotimes_{j=1}^{n-1} |\sigma_{n-1}(j)\rangle \right) |0\rangle_a^{\otimes(m+1)} \right] \\
& = \sum_{\sigma_{n-1} \in HC_{n-1}} \sum_{i=1}^{n-1} \frac{1}{\sqrt{(n-1)!}} |i\rangle \otimes \left(\bigotimes_{j=1}^{n-1} |\sigma_{n-1}(j) \oplus_0 i\rangle \right) |0\rangle_a^{\otimes(m+1)} \\
& = \sum_{\sigma_{n-1} \in HC_{n-1}} \sum_{t=1}^{n-1} \frac{1}{\sqrt{(n-1)!}} |\sigma_{n-1}(t)\rangle \otimes \left(\bigotimes_{j=1}^{n-1} |\sigma_{n-1}(j) \oplus_0 \sigma_{n-1}(t)\rangle \right) |0\rangle_a^{\otimes(m+1)} \\
& = \sum_{\sigma_{n-1} \in HC_{n-1}} \sum_{t=1}^{n-1} \frac{1}{\sqrt{(n-1)!}} |\sigma_{n-1}(t)\rangle \otimes \left(\bigotimes_{j=1}^{t-1} |\sigma_{n-1}(j)\rangle \right) |0\rangle_a^{\otimes m} \left(\bigotimes_{j=t+1}^{n-1} |\sigma_{n-1}(j)\rangle \right) |0\rangle_a^{\otimes(m+1)}. \tag{40}
\end{aligned}$$

By **Lemma 2**, we obtain the state

$$\sum_{\sigma_n \in HC_n} \frac{1}{\sqrt{(n-1)!}} |\sigma_n\rangle |0\rangle_a^{\otimes(m+1)}. \tag{41}$$

Now, we analyze the gate complexity. G_k in U_1 can be regarded as the amplitude amplification

method [36] and expanded as

$$G_k(\phi, \varphi) |0\rangle^{\otimes u} = (H^{\otimes u} S_0(\phi) H^{\otimes u} S_\chi(\varphi))^p H^{\otimes u} |0\rangle^{\otimes u} = \sum_{i=1}^{k-1} \frac{1}{\sqrt{k-1}} |i\rangle, \quad u = \lceil \log_2 k \rceil, \quad (42)$$

$$S_0(\phi) |j\rangle = \begin{cases} \exp(i\phi) |j\rangle, & j = 0 \\ |j\rangle, & j \neq 0 \end{cases}, \quad S_\chi(\varphi) |j\rangle = \begin{cases} \exp(i\varphi) |j\rangle, & 1 \leq j \leq k-1 \\ |j\rangle, & j = 0 \text{ or } k \leq j < 2^u \end{cases}. \quad (43)$$

We adopt three dimensional rotation form according to [35]:

$$p = \lceil \frac{\pi}{4 \arcsin \sqrt{(k-1)/2^u}} - \frac{1}{2} \rceil, \quad \phi = \varphi = 2 \arcsin \frac{\sin \frac{\pi}{4p+2}}{\sqrt{(k-1)/2^u}}. \quad (44)$$

Both $S_0(\phi)$ and $S_\chi(\varphi)$ can be implemented using $O(u)$ gates, via a technique called phase kick-back [8, 19]. $p = O(\sqrt{2^u/(k-1)}) = O(2)$ for $u \leq \log_2 k + 1$ and $k > 2$. Hence, U_1 requires the gate complexity of $O(pu) = O(\log_2 k)$. By **Lemma 4**, U_2 requires the gate complexity of $O((k-1)m) = O(k \log_2 n)$. In (37), $\bar{C}_j^m X_a$, $C_a X_j(k)$ and $C_j(k) X_a$ require $O(m)$ elementary gates, which yields a complexity of $O((k-1)m) = O(k \log_2 n)$ for (37).

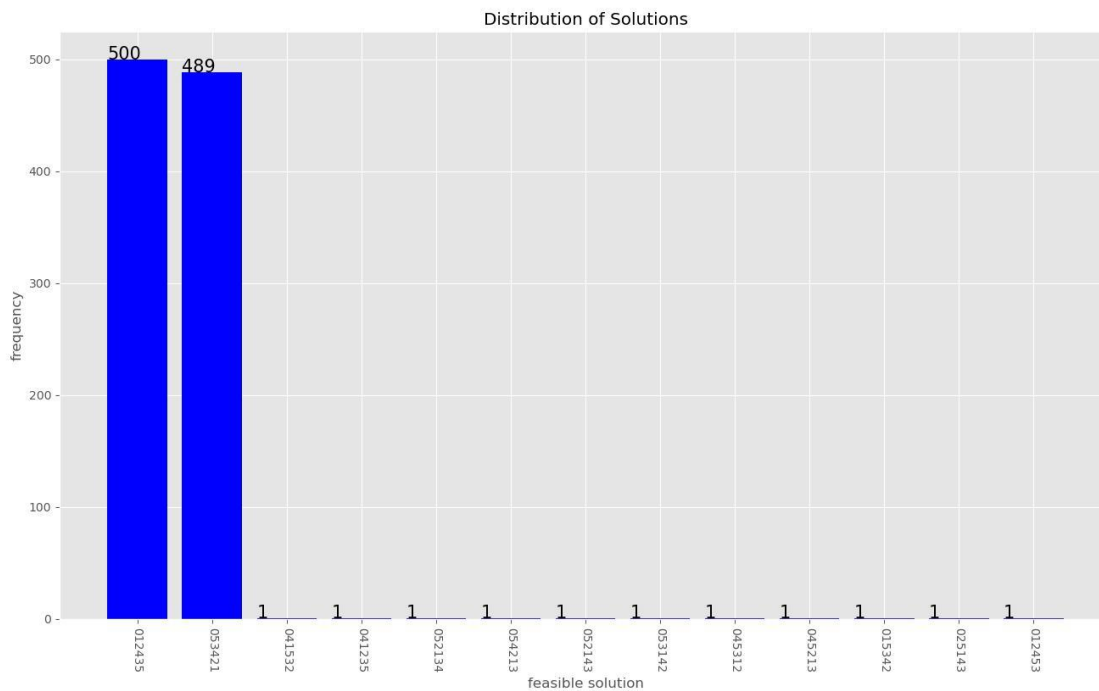
Collecting all the above complexities, our algorithm to prepare the uniform superposition state of Hamiltonian cycles of length n requires the gate complexity of $O(\sum_k (\log_2 k + k \log_2 n + k \log_2 n)) = O(n^2 \log_2 n)$.

Comparing **Lemma 3** with **Lemma 2**, we just need to modify two places for case of permutation. One is the initial state, which should be changed to $|0\rangle^{\otimes m} |1\rangle |0\rangle^{\otimes (n-2)m} |0\rangle_a^{\otimes (m+1)}$. The other is G_k , which should be changed to

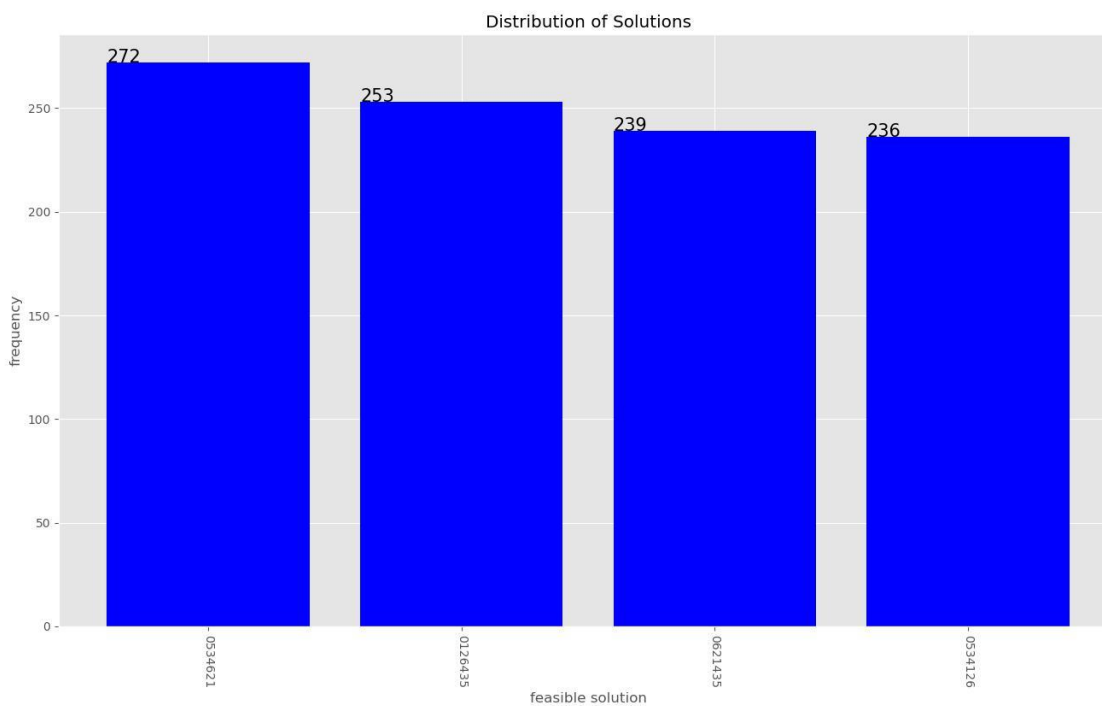
$$G_k(\phi, \varphi) |0\rangle^{\otimes u} = (H^{\otimes u} S_0(\phi) H^{\otimes u} S_\chi(\varphi))^p H^{\otimes u} |0\rangle^{\otimes u} = \begin{cases} \sum_{i=1}^k \frac{1}{\sqrt{k}} |i\rangle, & 2 \leq k < n \\ \sum_{i=0}^{n-1} \frac{1}{\sqrt{k}} |i\rangle, & k = n \end{cases},$$

where $u = \lceil \log_2(k+1) \rceil$ for $2 \leq k < n$ and $u = \lceil \log_2 n \rceil$ for $k = n$. The extra component in the superposition state compared to (42) precisely contributes to the additional permutation σ_k in **Lemma 3**. Similar to (44), $p = O(\sqrt{2^u/k}) = O(2)$ for $u \leq \log_2(k+1) + 1$ and $k \geq 2$. Therefore, this algorithm maintains the same complexity for the case of permutation. \square

I. The simulation verification results of our TSP solver.



(a) Result of graph with $n = 6$.



(b) Result of graph with $n = 7$.

FIG. A10: The simulation verification results of our TSP solver. The feasible solutions are represented by paths. For example, 012435 represents a route $0 \rightarrow 1 \rightarrow 2 \rightarrow 4 \rightarrow 3 \rightarrow 5 \rightarrow 0$. The bars with significant proportions are all optimal solutions.

-
- [1] Ambainis, A. *et al.* Quantum speedups for exponential-time dynamic programming algorithms. In *Proceedings of the Thirtieth Annual ACM-SIAM Symposium on Discrete Algorithms (SODA)*, 1783–1793 (SIAM, 2019).
 - [2] Bellman, R. Dynamic programming treatment of the travelling salesman problem. *Journal of the ACM (JACM)* **9**, 61–63 (1962).
 - [3] Chauhan, C., Gupta, R. & Pathak, K. Survey of methods of solving tsp along with its implementation using dynamic programming approach. *International journal of computer applications* **52** (2012).
 - [4] Laporte, G. The traveling salesman problem: An overview of exact and approximate algorithms. *European Journal of Operational Research* **59**, 231–247 (1992).
 - [5] Eppstein, D. The traveling salesman problem for cubic graphs. *Journal of Graph Algorithms and Applications* **11**, 61–81 (2007).
 - [6] Moylett, A. E., Linden, N. & Montanaro, A. Quantum speedup of the traveling-salesman problem for bounded-degree graphs. *Physical Review A* **95**, 032323 (2017).
 - [7] Ge, Y. & Dunjko, V. A hybrid algorithm framework for small quantum computers with application to finding hamiltonian cycles. *Journal of Mathematical Physics* **61** (2020).
 - [8] Lee, C. M. & Selby, J. H. Generalised phase kick-back: the structure of computational algorithms from physical principles. *New Journal of Physics* **18**, 033023 (2016).
 - [9] Ossorio-Castillo, J., Pastor-Díaz, U. & Tornero, J. M. A generalisation of the phase kick-back. *Quantum Information Processing* **22**, 143 (2023).
 - [10] Quek, Y., Canonne, C. & Rebentrost, P. Robust quantum minimum finding with an application to hypothesis selection. *arXiv preprint arXiv:2003.11777* (2020).
 - [11] Andrés-Martínez, P. & Heunen, C. Weakly measured while loops: peeking at quantum states. *Quantum Science and Technology* **7**, 025007 (2022).
 - [12] Burke, J. & McGoldrick, C. Deterministic quantum search via recursive oracle expansion. *arXiv preprint arXiv:2507.15797* (2025).
 - [13] Mascarenhas, L., Lula-Rocha, V. N. & Trindade, M. A. Quantum classification and search algorithms using spinorial representations. *arXiv preprint arXiv:2603.16564* (2026).
 - [14] Bai, X. & Shang, Y. A quantum speedup algorithm for tsp based on quantum dynamic programming with very few qubits. *Theoretical Computer Science* 115423 (2025).
 - [15] Gilliam, A., Woerner, S. & Gonciulea, C. Grover adaptive search for constrained polynomial binary optimization. *Quantum* **5**, 428 (2021).
 - [16] Marsh, S. & Wang, J. B. Combinatorial optimization via highly efficient quantum walks. *Physical Review Research* **2**, 023302 (2020).
 - [17] Bärttschi, A. & Eidenbenz, S. Grover mixers for qaoa: Shifting complexity from mixer design to state preparation. In *2020 IEEE International Conference on Quantum Computing and Engineering (QCE)*, 72–82 (IEEE, 2020).
 - [18] Jiang, J.-R. Dicke state quantum search for solving the vertex cover problem. *Mathematics* **13**, 3005 (2025).
 - [19] Chiew, M., de Lacy, K., Yu, C.-H., Marsh, S. & Wang, J. B. Graph comparison via nonlinear quantum search. *Quantum Information Processing* **18**, 302 (2019).
 - [20] Zhang, X.-M., Li, T. & Yuan, X. Quantum state preparation with optimal circuit depth: Implementations and applications. *Physical Review Letters* **129**, 230504 (2022).
 - [21] Held, M. & Karp, R. M. A dynamic programming approach to sequencing problems. *Journal of the Society for Industrial and Applied mathematics* **10**, 196–210 (1962).
 - [22] Grover, L. K. A fast quantum mechanical algorithm for database search. In *Proceedings of the twenty-eighth annual ACM symposium on Theory of computing*, 212–219 (1996).
 - [23] Zhu, J., Gao, Y., Wang, H., Li, T. & Wu, H. A realizable gas-based quantum algorithm for traveling salesman problem. *arXiv preprint arXiv:2212.02735* (2022).
 - [24] Sattolo, S. An algorithm to generate a random cyclic permutation. *Information processing letters* **22**, 315–317 (1986).
 - [25] Wilson, M. C. Overview of sattolo’s algorithm. In *Algorithms Seminar, 2002–2004*, 105 (2005).

- [26] Fisher, R. A. & Yates, F. Statistical tables for biological, agricultural and medical research. (1957).
- [27] Binkowski, L. & Schwiering, M. Quantum fisher-yates shuffle: Unifying methods for generating uniform superpositions of permutations. *arXiv preprint arXiv:2504.17965* (2025).
- [28] Cain, M. *et al.* Shor’s algorithm is possible with as few as 10,000 reconfigurable atomic qubits. *arXiv preprint arXiv:2603.28627* (2026).
- [29] Durr, C. & Hoyer, P. A quantum algorithm for finding the minimum. *arXiv preprint quant-ph/9607014* (1996).
- [30] Boyer, M., Brassard, G., Høyer, P. & Tapp, A. Tight bounds on quantum searching. *Fortschritte der Physik: Progress of Physics* **46**, 493–505 (1998).
- [31] Shen, F. *et al.* A bucket-brigade quantum random access memory. *Nature Physics* 1–6 (2026).
- [32] Dicke, R. H. Coherence in spontaneous radiation processes. *Physical review* **93**, 99 (1954).
- [33] Bärtschi, A. & Eidenbenz, S. Deterministic preparation of dicke states. In *International Symposium on Fundamentals of Computation Theory*, 126–139 (Springer, 2019).
- [34] Gidney, C. Constructing large controlled nots. *Algorithmic Assertions* (2015). URL <https://algassert.com/circuits/2015/06/05/Constructing-Large-Controlled-Nots.html>.
- [35] Long, G.-L. Grover algorithm with zero theoretical failure rate. *Physical Review A* **64**, 022307 (2001).
- [36] Brassard, G., Hoyer, P., Mosca, M. & Tapp, A. Quantum amplitude amplification and estimation. *arXiv preprint quant-ph/0005055* (2000).